MECHANISMS OF PREDICTION AND POTENTIAL CAUSATION OF ORGANOPHOSPHATE INDUCED DELAYED NEUROTOXICITY

by

Nichole DeEtta Hein

A dissertation submitted in partial fulfillment
of the requirements for the degree of
Doctor of Philosophy
(Toxicology)
in The University of Michigan
2009

Doctoral Committee:

Professor Rudy J. Richardson, Chair
Professor Paul F. Hollenberg
Associate Professor Peter Mancuso
Research Assistant Professor Jeanne Stuckey

To my sunshine - Daphne Louise

ACKNOWLEDGEMENTS

I am absolutely appreciative of the opportunity to study and grow in the Toxicology Program of the Department of Environmental Health Sciences in the University of Michigan. The work that has been completed herein could not have been accomplished without the invaluable teachings of the faculty and support from the staff.

I would like to thank Dr. Rudy Richardson for inviting me into his laboratory to work and learn, and for his guidance, patience, and support as I completed this program.

I am grateful for the advice and direction provided by my committee members Dr. Rudy Richardson, Dr. Jeanne Stuckey, Dr. Paul Hollenberg, and Dr. Peter Mancuso.

I also extend a thank you to Jen Pierce and Dr. Tim Kropp who introduced me to the laboratory and helped me initiate the work that I would continue. In addition, I would like to thank Dr. Rob Christner for his guidance on the SELDI TOF-MS.

I need to thank Dr. Jeanne Stuckey and the members (former and current) of her laboratory, Pat Gee, Ann Kendall, Dr. Jen Meagher, and Dr. Ron Rubin at the Life Sciences Institute for their assistance in the production of NEST and the mutations, without whom much of this work would not have been completed.

I would like to thank Dr. Steve Bursian and Angelo Napolitano who provided the source of hen brain enzymes from the poultry research and training center at Michigan State University. In addition I would like to thank Dr. John Fink and Dr. Shirley Rainier

for providing the source of mouse brain enzymes and for discovering the mutations that led to the work in Chapter 4 of the dissertation.

I would like to thank the researchers from the Institute of Physiologically Active Compounds in Chernogolovka, Russia, particularly Dr. Galina Makhaeva, who provided the fluorinated aminophosphonate compounds.

I want to include a word of appreciation to all of the other students, my friends, and my family that have supported me through this journey.

Finally, I acknowledge the support of the U.S. Army Research Office grant number DAAD19-02-1-0388, Pharmaceutical Sciences Training Program, Environmental Toxicology Training Program Grant NIH ES07062, Dow Chemical Company, Dow Agrosciences, AstraZeneca Pharmaceuticals, and Dr. Martin Philbert and Dr. Rita Loch-Caruso for providing the funding or materials that allowed me to complete my research.

TABLE OF CONTENTS

LIST OF TABLES

LIST OF FIGURES

LIST OF ABBREVIATIONS

° C	degree Celsius
>	greater than
µL	microliter
µM	micromolar
2-PAM	pyridine-2-aldoxime methiodide
4-AAP	4-aminoantipurine
ACh	acetylcholine
AChE	acetylcholinesterase
ACN	acetonitrile
ADME	absorption, distribution, metabolism, and excretion
ANOVA	analysis of variance
ATCh	acetylthiocholine
BChE	butyrylcholinesterase
BTCh	butyrylthiocholine
Ca	Calcium
CHAPS	3-[(3-cholamidopropyl)dimethylammonio]-1-propanesulfonate
CHCA	α-cyano-4-hydroxycinnamic acid
CO_2	carbon dioxide

C—P	carbon-phosphorus bond
CPO	O,O-diethyl O-3,4,5-trichloro-2-pyridyl phosphate, chlorpyrifos oxon
CPS	diethyl 3,5,6-trichloro-2-pyridyl phosphorothionate, chlorpyrifos, Dursban
Da	daltons
DFP	diisopropylphosphorofluoridate
DMF	*N,N′* dimethylformamide
DMSO	dimethyl sulfoxide
DNA	deoxyribonucleic acid
DOPC	dioleoylphosphatidylcholine
DTNB	5,5′-dithio-bis(2-nitrobenzoic acid)
EDTA	ethylenediaminetetraacetic acid
EOH	serine esterase
EOP	phosphylated serine esterase
EOP_{aged}	aged phosphylated serine esterase complex
FAP	fluorinated aminophosphonate
g	force of gravity
GA	tabun
GB	sarin
GD	soman
GPC	glycerophosphocholine
h	hour, hr
hb	hen brain

HCl	hydrochloric acid
hr	human recombinant
hs	horse serum
IPTG	isopropyl-β-D-thiogalctopyranoside
k_4	unimolecular rate of aging
KCl	potassium chloride
KF	potassium fluoride
k_i	bimolecular rate of inhibition
Km	Michaelis constant
kV	kilovolts
LB	media containing salt, tryptone, and yeast extract
LPC	lysophosphatidylcholine
M	molar
m/v	mass per charge
M1012V	methionine to valine mutation at residue 1012
mb	mouse brain
MH^+	protonated molecule
min	minute
MIP	*N*,*N*′-diisopropylphosphorodiamidofluoridate, mipafox
mM	millimolar
NaCl	sodium chloride
NEST	human recombinant NTE esterase catalytic domain

ng	nanograms
nm	nanometer
NMR	nuclear magnetic resonance
ns	nanosecond
NTE	neuropathy target esterase
NTE-MND	NTE-related motor neuron disease
NZY^+	an enriched broth containing casein hydrolysate amine, yeast extract, glucose and magnesium salts
OP	organophosphorus
OPIDN	OP compound-induced delayed neurotoxicity
PC	phosphatidylcholine
PMSF	phenylmethylsulfonyl fluoride
PV	phenyl valerate
PX	OP compound with leaving group X
R890H	arginine to histidine mutation and residue 890
RIP	relative inhibitory potential
RNA	ribonucleic acid
SDS	sodium dodecyl sulfate
sec	second
SELDI-TOF MS	surface enhanced laser desorption/ionization time-of-flight mass spectrometry
SEM	standard error mean
S_N2	bimolecular nucleophilic substitution
sws	swiss cheese, NTE gene homologue in *Drosophila*

t	time
TFA	trifluoroacetic acid
v/v	volume per volume
w/v	weight per volume
w/w	weight per weight

ABSTRACT

Organophosphorus (OP) compounds, used in insecticides, pharmaceuticals, and weapons of biochemical warfare inhibit serine hydrolases. Exposure to OP compounds has shown that a phosphylation of certain serine esterases results in two distinct types of toxicities: an acute cholinergic toxicity associated with inhibition of acetylcholinesterase (AChE), and a more chronic toxicity associated with the inhibition and aging of neuropathy target esterase (NTE). OP induced delayed neurotoxicity (OPIDN) occurs when a threshold of NTE is inhibited and aged, and is characterized by axonopathies in the peripheral and central nervous systems 1-4 weeks after exposure. An accurate *in vivo* model of OPIDN is difficult to develop, due to interspecies variations of inhibitor sensitivity and metabolism. Understanding the mechanism of inhibition and aging of serine esterases by OP compounds and correlating this with pathological axonopathies are important for research on OPIDN.

Fluorinated aminophosphonates (FAP) are a group of OP compounds that were hypothesized to inhibit serine esterases through a scission in a chemically stable carbon-phosphorus bond. Through the use of surface enhanced laser desorption/absorption time of flight mass spectrometry, the FAP compounds were shown to covalently phosphorylate the active site serine of butyrylcholinesterase and subsequently age through dealkylation.

To begin modeling OPIDN, correlations were found in the bimolecular rate constants of inhibition of AChE and NTE using hen brain, mouse brain, and human recombinant enzymes. Furthermore, correlations in relative inhibitory potentials were found that could predict the neuropathic potential of OP compounds.

Finally, two point mutations in NTE were found in patients with a hereditary spastic paraplegia that had clinical presentations similar to OPIDN. Through site-directed mutagenesis, these mutations were created in the catalytic domain of NTE and found to have altered enzymological properties, including reduced kinetic rates of substrate hydrolysis, inhibition, and aging.

This research reveals that the mechanism of inhibition by OP compounds can be elucidated using mass spectrometry. Additionally, associations of kinetic values between rodents, hens, and humans may lead to further modeling of OPIDN. In conclusion, alterations in the enzymological properties of NTE may be associated with pathology presented in patients with and associated motor neuron disease.

CHAPTER 1

BACKGROUND AND INTRODUCTION

Organophosphorus (OP) compounds are esters of phosphorous or phosphonic acid and therefore contain either trivalent or pentavalent phosphorus. The mechanism of toxicity elicited by trivalent phosphorus appears to be different from that of the pentavalent form in both mechanistic and clinical perspectives (Abou-Donia, 1992). The general structure of pentavalent OP compounds can be seen in Figure 1.1, and it is this form that will be discussed herein. Although the most studied interactions with OP compounds is with acetylcholinesterase (AChE), there are over 1000 serine hydrolases identified in humans whose physiology is mostly unstudied (Casida and Quistad, 2005).

History of Organophosphorus Compounds

The first reported OP synthesis was of tetraethylpyrophosphate by Phillipe de Clermont in 1854 (Karczmar, 1998). Investigations of OP compounds continued as they were discovered to be toxic to both humans and insects, and this use has led to their widespread development as anti-cholinesterase agents. During World War II, German chemist Gerhard Schrader began synthesis and marketing of OP compounds as potent insecticides, and due to their toxic nature, further developed them as military warfare

agents (Holmstedt, 1959). He is credited with the development of the first OP insecticides parathion, chlorthion, and fenthion, as well as the extremely toxic G-series of nerve agents sarin (GB), soman (GD), and tabun (GA), which are still a threat to public health today.

In 1941, British scientists McCombie and Sunders reported their synthesis of diisopropylphosphorofluoridate (DFP), and further noted its cholinergic and even latent neurological effects (Saunders and Stacy, 1948; Saunders, 1957). Ten years later, a brief news statement was made in the journal *Nature* about a new pesticide, *bisiso*propyl-amino-fluorophosphine oxide (mipafox) that has "one twenty-sixth" the toxicity of parathion (Anonymous, 1951). The latent paralysis clinically presenting two weeks following exposure to mipafox would later be compared to paralysis following other documented OP exposures, and suggested further animal research to investigate this associated pathology (Bidstrup *et al.*, 1953). In 1965, Dow commercialized the insecticide diethyl 3,5,6-trichloro-2-pyridyl phosphorothionate (chlorpyrifos, Dursban), which had potent anti-cholinergic properties (Richardson, 1995). It was later discovered that chlorpyrifos, when actively metabolized to the oxon form, can cause a delayed neurotoxicity, when the cholinergic symptoms are effectively treated (Capodicasa, 1991). The chemical structures of these highlighted OP compounds can be seen in Figure 1.2.

Fluorinated Aminophosphonates

OP compounds may be found to cause anti-cholinergic or neuropathic symptoms, but the mechanism and interaction with the target is poorly understood. A group of fluorinated aminophosphonates (FAP) compounds (Figure 1.3) was found to inhibit

serine esterases *in vitro* (Makhaeva *et al.*, 2005). These compounds are unique, because they do not possess the typical sort of leaving group that can usually be identified in OP inhibitors of esterases. The lack of a standard electrophilic leaving group requires that the covalent binding of the phosphoryl moiety, phosphylation, of the serine esterase break a carbon-phosphorus (C—P) bond, which is biochemically a stable, nonreactive bond (Quinn *et al.* 2007). Molecular modeling and X-ray crystallography reveal that the C—P bond in FAP compounds is made longer and weaker by the adjacent trifluoromethyl groups, supporting the hypothesis that FAP compounds inhibit serine esterases via covalent phosphylation involving a break in the C—P bond (Chekhlov *et al.*,1995; Makhaeva *et al.*, 2005; Wijeyesakere *et al.*, 2008). These studies also revealed that these compounds exist as hydrogen-bonded dimers, in which the sulfonamido hydrogen on one FAP molecule is paired with the phosphoryl oxygen of the other molecule. FAP compounds should be in monomeric form to make the C—P bond accessible before they are able to phosphylate the active site serine; however, direct experimental tests of this hypothesis have been lacking.

The study of OP compound toxicity is relevant today, as these compounds have been developed for use as insecticides, fungicides, lubricants, hydraulic fluids, plasticizers, flame retardants, fuel additives, pharmaceuticals, and weapons of biochemical warfare or terrorism. Although their use is declining, in 2000, over half the world market for pesticides consisted of anticholinergic OP compounds or the similarly acting carbamates (Nauen and Bretschiner, 2002).

Mechanism of OP Toxicity

Interactions of OP compounds with serine hydrolases occurs through reversible formation of a Michaelis-type intermediate before covalent phosphylation of the active site serine. This entire forward process, described as inhibition is a concentration- and time-dependent process, which is derived as follows (Aldrige and Reiner, 1972). The interaction of OP compounds and serine containing esterases/lipases is classically described by the reaction seen in Figure 1.4.

The [PX] required for half the maximum rate of production of EOP and HX or the maximum rate of regeneration of EOH can be described by the Michaelis constant (K_m) as shown below.

$$K_m = \frac{k_{-1} + k_2}{k_{+1}} - \frac{k_3}{k_2 + k_3}$$

The constant (K_a) which describes inhibition is shown:

$$K_a = \frac{k_{-1} + k_{+2}}{k_{+1}}$$

The K_a describes [PX] that is required to achieve a half-maximal rate of EOP, and is rarely described for substrates, as their distinction from inhibitors is that they quickly reactivate to EOH. K_a is related to k_2 and the bimolecular rate constant of inhibition (k_i) by

$$k_i = \frac{k_2}{K_a}$$

This relationship assumes only a small amount of the Michaelis complex is present. Determination of k_i, k_2, and K_a is done by solving the differential equation that describes the overall rate of inhibition:

$$\ln v_o - \ln v_t = \frac{k_2[PX]}{[PX] + K_a} t_i$$

where v_o is the rate of enzyme activity in the absence of PX, v_t is the activity of the inhibited enzyme at time t, t_i is the time of inhibition.

In the case of OP compounds with serine esterases, [EOH•PX] and k_3 are small. The preceding differential equation can then be simplified to

$$\ln v_o - \ln v_t = k_i[PX]t_i$$

Since ln v_t is a linear function of t_i, this can be used to plot of ln v_t against t_i at a specified [PX]. This plot creates a line with a slope equal to the first order rate constant of inhibition (k') that can be described by

$$k' = ki[PX]$$

Using several [PX], the slope of a secondary plot of k´ against [PX] is the k_i. It should be noted, this simpler equation does not allow for a determination of k_2 or K_a. Moreover, it is important to realize that in the determination of k_i, near-equilibration models of pseudo first-order kinetic rates are used, since secondary binding sites of serine esterases by increasing [PX] may inaccurately decrease the value (Rosenfeld and Sultatos, 2006).

Subsequently, the esterase may be reactivated through a nucleophilic displacement with water, or other nucleophile. If the OP compound contains a phosphoester or phosphoramidate, the OP-esterase complex may also undergo a post-inhibitory process of aging, which leads to a nonreactivatable enzyme.

The rate of aging is determined by the first-order equation

$$\ln(\%\text{reactivation}) = k_4 \cdot t_{aging}$$

The % reactivation is described by

$$\%\text{reactivation} = \frac{(AR_t) - (AI_t)}{(AR_0) - (AI_0)} x100$$

where AR_t is the activity of reactivated enzyme at t_{aging}, AR_0 is the activity of reactivated enzyme at t_0; AI_t is the activity of inhibited enzyme without reactivator at t_{aging}; and AI_0 is the activity of inhibited enzyme without reactivator at t_0. A plot of ln (100/% reactivation) against t_{aging} has a linear slope from which the rate of aging (k_4) is calculated.

Aging can occur by net removal of an alkyl/alkyl group from an ester, or deprotonation of a phosphoramidate nitrogen, from the OP moiety on the organophosphylated enzyme; the aged enzyme cannot be reactivated spontaneously or via nucleophilic displacement, permanently blocking normal function (Kropp and Richardson, 2006).

Acute OP toxicity

The cholinesterases, AChE and pseudocholinesterase, or butyrylcholinesterase (BChE) are serine esterases that belong to the α/β hydrolase fold family (Cygler *et al*., 1993). Crystallographic structures show that the cholinesterases contain the catalytic triad Ser-His-Glu, which is located at the bottom of a deep gorge lined with aromatic residues (Sussman *et al*, 1991, Ngamelue *et al.*, 2007). These esterases hydrolyze acetylcholine (ACh) through an S_N2 attack of the hydroxyl group in the active site serine on the carbonyl carbon of ACh. This hydrolysis is the biological function of AChE found in the cholinergic synapses and neuromusculature of the central and peripheral nervous systems. Although, also found in the synaptic space, BChE cannot overcome the requirements of ACh hydrolysis to maintain survival of $AChE^{-/-}$ mice (Chattonet *et al.*

2003). AChE found in circulating erythrocytes and BChE, which is found in circulating plasma, have no known physiological function, although they can hydrolyze ACh and other esters, and may serve to bind exogenous toxins and as biomarkers of exposure to esterase inhibitors (Nicolet *et al*., 2003).

The anti-cholinergic toxicity of OP compounds is highly relevant because many of them are non-specific to insect or mammals, including humans (Lotti and Johnson, 1978). OP compounds phosphylate the active site serine inhibiting the necessary hydrolysis of ACh. Acute OP toxicity is due to the inhibition of synaptic AChE and the subsequent buildup of ACh in the central and/or peripheral nervous systems (Thompson and Richardson, 2004). With an overabundance of ACh in the synapse, muscarinic and/or nicotinic receptors of cholinergic neurons become over stimulated. Signs and symptoms associated with muscarinic toxicity include salivation, lacrimation, urination, diarrhea, perspiration, bradycardia, bronchorrea, pallor, abdominal cramps, and miosis (Bajgar, 2004). Those associated with nicotinic toxicity include muscle fasciculations, weakness, paralysis, hypertension, tachycardia, and mydriasis. If untreated, these cholinergic toxicities can lead to respiratory failure, coma, and death.

Several treatments can be given for OP intoxication. These can be effective but are often inefficient. Pyridostigmine bromide administered before or directly after an OP exposure will carbamylate uninhibited AChE, but because the carbamylated enzyme spontaneously reactivates relatively quickly, pyridostigmine can prevent phosphorylation and permit AChE activity to be restored. If AChE has already been phosphorylated but not aged, a mixture of obidoxime and pralidoxime can be given; these oximes regenerate AChE activity through nucleophilic displacement of the phosphyl moiety from the

AChE-OP complex (Russel *et al.*, 2003). Another treatment given for OP intoxication is the cholinolytic drug atropine, which blocks the muscarinic acetylcholine receptor and lessens the muscarinic toxicities; however, the nicotinic effects must still be monitored (Wilson, 1984). Pyridostigmine bromide and atropine may be given to treat all OP intoxications; however oximes are only effective in the peripheral nervous system and if administered before aging of inhibited AChE occurs, because the aged complex cannot be reactivated. Thus, oximes can be effective against slowly aging diethyl phosphates found in many OP insecticides, but not against nerve agents such as sarin or soman, which age rapidly.

Chronic OP toxicity

Survival of the acute toxicities of certain OP compound exposures may permit the expression of a chronic non-cholinergic toxicity, characterized by degeneration of the long axons in sensory and motor neurons in the peripheral nervous system and spinal cord. This syndrome, called OP compound-induced delayed neurotoxicity (OPIDN) is strongly associated with the inhibition of NTE by OP compounds and the subsequent aging of the NTE-OP complex.

NTE inhibitors can be divided into two functional classes depending on their biological effects (Davis and Richardson, 1980). Type A, also called neuropathic NTE inhibitors consist of certain phosphates, phosphonates, and phosphorodiamidates; the NTE adducts of these compounds can all undergo the aging reaction, which entails loss of a ligand or proton from the phosphyl moiety to generate a negative charge. This process, called aging, occurs within minutes, leaving NTE refractory to reactivation

(Clothier and Johnson, 1980). Type B, or non-neuropathic NTE inhibitors include certain phosphinates, sulfonates, and carbamates; the NTE adducts of these compounds cannot undergo aging, and in fact may protect from neuropathic lesions (Johnson, 1970). The basic structures of these classes of compounds can be seen in Figure 1.5.

NTE is an integral membrane protein, which has an apparent weight of 155kDa due to glycosylation, and a molecular weight of 146 kDa. NTE is not localized within a particular area of a cell; however, it is most prevalent in large neurons with abundant rough endoplasmic reticulum (Glynn *et al*., 1998). NTE activity is operationally defined by phenyl valerate hydrolysis that is not inhibited by paraoxon, but is abolished by mipafox (Johnson, 1969). There are three *N*-terminal putative cyclic nucleotide-binding domains, which thus far have not been shown to bind to nucleotides (Li *et al.*, 2003). The C-terminal 200 amino acid sequence in human NTE containing the active site serine is homologous to conceptual proteins predicted from gene sequences in chicken, *Drosophila*, mice, *C. elegans*, yeast, *E. coli*, and *M. tuberculosis* (Lush *et al*., 1998). Although there are no crystallographic data, bioinformatics and modeling suggest that the catalytic domain of NTE may be related to patatin and the Ca-independent phospholipase A2 enzymes (Glynn, 2006; Wijeyesakere *et al*., 2007). By function, NTE has been classified as a lysophospholipase, because of its ability to hydrolyze lysophosphatidylcholine (LPC), and to deacylate phosphatidylcholine (PC) to glycerophosphocholine (GPC) (van Tienhoven *et al*., 2002; Quistad *et al.*, 2003; Zaccheo *et al*., 2004). Exposures of high levels of LPC are neurotoxically associated with demyelination in mice (Hall, 1972). Expression of NTE in a cellular model has been shown to protect against LPC toxicity (Vose *et al.*, 2008).

This neuropathic toxicity is manifested when there is inhibition and aging of more than 70% NTE in the central and peripheral nervous systems (Johnson, 1982). Clinical observations manifest 1-4 weeks after exposure to a neuropathic OP compound, and are consistent with a Wallerian-type distal axonopathy, a wave-like and active process of proximal to distal degeneration (Beirowski *et al*., 2005). Symptoms include paresthesias in the distal extremities, sensory loss, ataxia, and flaccid paralysis. Eventual reinnervation of the muscle with persistent lesions in descending upper motor neuron axons can lead to spastic paralysis. Moreover, OP compounds that are not effective inhibitors of AChE, but that are potent inhibitors of NTE, can produce OPIDN in the absence of acute cholinergic signs or symptoms. Although in mild cases of OPIDN, there can be recovery of motor and sensory function; there are no effective treatments (Lotti and Moretto, 2005)

Modeling of OPIDN

There is a large gap of knowledge about the pathophysiological processes that occur between exposure to a neuropathic OP toxicant and the development of OPIDN. Very little is understood about the molecular mechanism involved once the aged NTE-OP complex occurs and leads to distal degeneration of axons in peripheral nerves and/or spinal cord tracts. Ignorance of these processes is partly due to a lack of model, either *in vivo* or *in vitro* that is reasonable for elucidating OPIDN. The current *in vivo* model for production of OPIDN following OP exposure is in adult chickens (usually hens). There has been a large effort to understand the role of NTE, to elucidate the events following

inhibition and aging of the OP-NTE complex, and to create a more efficient model that would characterize the disease progression in humans (Pomeroy-Black *et al.*, 2007).

Several methods have been used to understand the function of NTE, including site-directed mutagenesis, cloning, and RNA interference. *S. cerevisiae* lacking *NTE1*, a yeast homologue to NTE, produces no intracellular glycerophosphocholine, leading to the hypothesis that NTE is necessary for the degradation of phosphatidylcholine as mentioned earlier. Differentiated neuroblastoma cells overexpressing recombinant NTE are able to overcome toxicities induced by high levels of introduced LPC (Vose, 2008). When Swiss cheese (*sws*), a homologous gene of NTE in *Drosophila*, is mutated, there is extensive vacuolization in the nervous system, and extensive neuronal and glial apoptosis (Kretzschmar *et al.*, 1997). Furthermore, $nte^{-/-}$ transgenic mice are embryonic-lethal on embryonic day 09 with gross morphological disruption due to a disruption in vasculogenesis (Moser *et al.*, 2004). Heterozygous conditional inactivation of NTE in mice causes a 40% decrease in NTE activity, with no neurodegeneration; however, double conditional NTE inactivation causes a 90% decrease in NTE activity and leads to neuronal vacuolization and accumulation of intracellular organelles (Akassoglou *et al.*, 2004). Proper function of the NTE protein and its homologues are necessary for cellular membrane integrity; however, there is a level of decreased activity that must be reached before neurodegeneration takes place.

Although gross morphological changes can be seen when deleting or mutating the entire gene, modeling OPIDN after exposure to an OP-compound is not so easily done. There are many differences in the clinical manifestations of OPIDN across vertebrate species. Chickens have long been the standard, because inhibition of NTE greater than

70% leads to the development of OPIDN 2-3 weeks after dosing, with central-peripheral distal axonopathies like those seen in humans (Johnson, 1990). These pathologies are difficult to model, however, due to differences between cholinergic and neuropathic thresholds, and in rates of metabolism of OP toxicants and protoxicants (Moretto and Lotti, 2002). Rats have been thought to be insensitive to OPIDN, because despite exposure to high levels of neuropathic compounds, they do not develop the classic hind-limb paralysis (Abou-Donia, 1981). Mice are even more difficult because of the inability to inhibit the threshold of 70% NTE (Veronesi *et al.*, 1991). Difficulty in correlating NTE inhibition with pathology in rodents has also been attributed to differences in aging and resynthesis of NTE, levels of esters in the brain, and axonal length.

In order to study the effects of critical residues within the NTE catalytic domain, the NTE-esterase domain (NEST) was expressed in *E. coli*, and purified. These studies have shown that certain mutations to the active site serine and two necessary aspartate residues within the esterase domain can abolish all activity (Atkins and Glynn, 2000). Mutations in the sequence of NEST, which lead to an OPIDN-like pathology, may also have measurable changes in the physiological properties (Rainier *et al.*, 2008). A recent neurogenetic evaluation revealed several people who were discovered to have three different types of a genetic autosomal recessive mutation in the locus encoding NTE. Two of these involved point mutations within NEST, and a third mutation, which was an insertion into a codon that caused a premature stop, and therefore a truncation. Patients with these mutations presented with lower extremity spastic weakness associated with wasting of distal upper and lower extremity muscles associated with distal motor

axonopathies. The clinical manifestations of the disease could be classified with a diagnosis of a hereditary spastic paraplegia, and also bears some similarity to OPIDN.

Hypotheses

Understanding the mechanism of inhibition and aging of serine esterases by novel compounds is important for research on OPIDN. Before rational preventatives and treatments can be developed for this type of chemical exposure, the mechanism of toxicity must first be elucidated. The purpose of this research is to develop an understanding of which compounds will have potential to cause OPIDN, and to elucidate a mechanism to predict this potential in humans.

(1) FAP compounds inhibit serine BChE through covalent phosphorylation through a break in the carbon-phosphorus bond. Moreover, the resultant OP-esterase complex subsequently ages through net loss of an alkyl group.

(2) Neuropathic compounds are those that cause OPIDN. Correlations in the bimolecular rate constants of inhibition and unimolecular rate constant of aging among mice, humans, and hens can be used in order to predict neuropathic potential within and across species.

(3) Mutations of NTE have been associated with pathological OPIDN-like degeneration of the long axons in motor neurons. These mutations, when created in recombinant NEST, will show a measurable alteration in catalytic properties.

Specific Aims

(1) The bimolecular rate constants of inhibition (k_i) for each of the FAP compounds and horse serum BChE (hsBChE) will be determined using kinetic experiments.

(2) The serine phosphorylation adducts of inhibited and aged FAP-esterase complexes will be identified for hsBChE, using surface enhanced laser desorption/ionization time-of-flight mass spectrometry (SELDI-TOF MS).

(3) The k_i and k_4 for a published series of compounds and hen and mouse brain AChE and NTE will be determined using *in vitro* kinetic experiments.

(4) The data from specific aim 3 will be used to calculate relative inhibitory potencies (RIPs) of the compounds, to compare the inhibitory and aging kinetics between the species.

(5) Human recombinant NEST mutants will be produced and expressed in an *E. coli* system, and the phenyl valerate hydrolase activity will be measured and compared with the native enzyme.

(6) Inhibitory and aging kinetics will also be used to evaluate possible changes in catalytic properties.

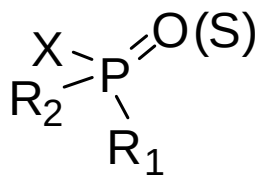

Figure 1.1. General structure of organophosphorus compounds. R_1 and R_2 are generally alkyl, alkoxy, or amidate structures, and X is the leaving group that is displaced upon phosphylation. The double bond could be either oxygen or sulfur.

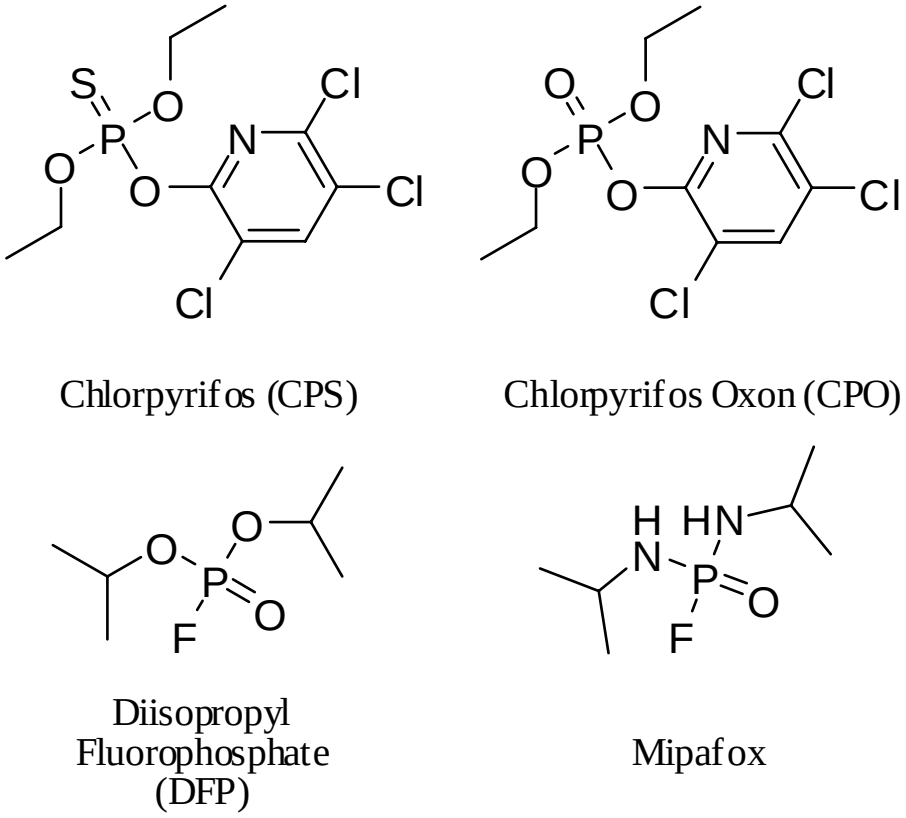

Figure 1.2. Chemical structure of CPS and the active oxon metabolite (CPO), DFP, and mipafox

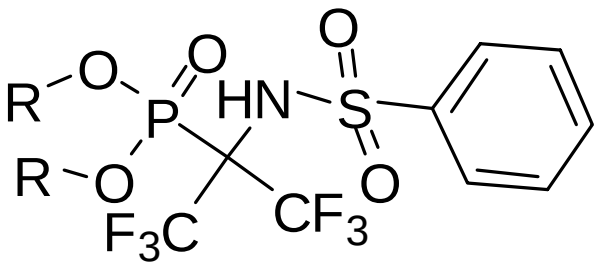

Figure 1.3. General structure of FAP compounds. R = alkyl groups that vary in length and branching.

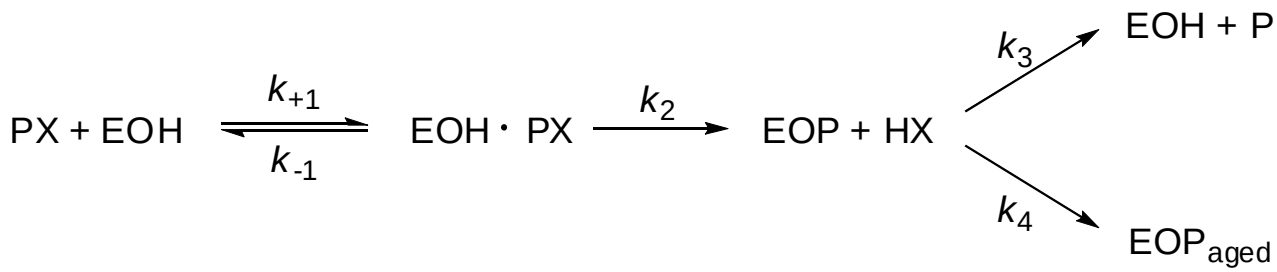

Figure 1.4. Interactions of OP compounds with serine esterases. PX is the OP compound with electrophilic leaving group X, EOH is the serine esterase, EOH-PX is the Michaelis-type intermediate, and EOP is the covalently phosphylated esterase. EOP can than either reactivate through hydrolysis to yield EOH, or age, as denoted by EOP_{aged}. The forward process into the formation of the Michaelis complex is described by the second order constant k_{+1}, and the reverse is described by the first order constant k_{-1}. The covalent formation of a phosphylated serine adduct is described by the first order constant k_2. The entire forward inhibitory process is described by the bimolecular rate of inhibition, k_i. The postinhibitory processes can either be described by the first order constant for reactivation, k_3, or the first order rate of aging k_4.

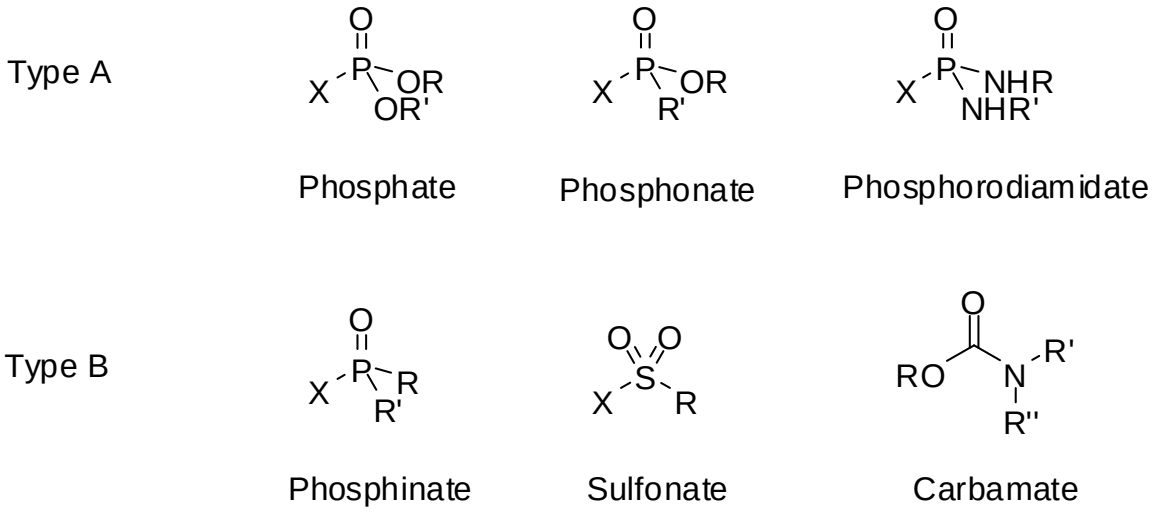

Figure 1.5. Basic structures and nomenclature of Type A and Type B NTE inhibitors. Alkyl groups are denoted by R, and leaving groups are denoted by X**.**

References

Anonymous (1951). A new systemic insecticide, *Nature* **167,** 260.

Abou-Donia, M.B. (1981). Organophosphorus ester-induced delayed neurotoxicity. *Annu. Rev. Pharmacol. Toxicol.* **21,** 511-548.

Abou-Donia, M. B. (1992). Tri-phenyl phosphite: a type II organophosphorus compound induced delayed neurotoxic agent. In *Organophosphates: Chemistry, Fate, and Effects* (J.E. Chambers and P.E. Levi, eds.), Academic Press, San Diego, pp. 327-351.

Aldridge, W.N., and Reiner, E. (1972). *Enzyme Inhibitors as Substrates: Interactions of Esterases with Esters of Organophosphorus and Carbamic Acids.* North-Holland Publishing, Amsterdam.

Akassoglou, K., Malester, B., Xu, J., Tessarollo, L., Rosenbluth, J., and Chao, M.V. (2004). Brain-specific deletion of neuropathy target esterase/swisscheese results in neurodegeneration. *PNAS.* **101,** 5075-5080.

Atkins, J., and Glynn, P. (2000). Membrane association of and critical residues in the catalytic domain of human neuropathy target esterase. *Biochem. J.* 275**,** 24477-24483.

Bajgar J. (2004). Organophosphates/nerve agent poisoning: mechanism of action, diagnosis, prophylaxis and treatment. *Adv. Clin. Chem.* **38,** 151-216.

Beirowski, B., Adalbert, R., Wagner, D., Grumme, D.S., Addicks, K., Ribchester, R.R., and Coleman, M.P. (2005). The progressive nature of Wallerian degeneration in wild-type and slow Wallerian degeneration (Wld^S) nerves. *BMC Neuroscience* **6,** 6-32.

Bidstrup, P.L, Bonnell, J.A., and Beckett, A.G. (1953). Paralysis following poisoning by a new organic phosphorus insecticide (mipafox). *Brit. Med. J.* 1068-1072.

Capodicasa, E., Scapellato, M.L., Moretto, A., Caroldi, S., and Lotti, M. (1991). Chlorpyrifos-induced delayed polyneuropathy. *Arch. Toxicol.* **65,** 150-155.

Chattonet, F., Boudinot, E., Chatonnet, A., Taysse, L., Dulon, S., Champagnat, J., and Foutz, A.S. (2003). Respiratory survival mechanisms in acetylcholinesterase knockout mouse. *Eur. J. Neurosci.* **18,** 1419-1427.

Chekhlov, A.N., Aksinenko, A.Y., Sokolov, V.B., and Martynov, I.V. (1995). Crystal and molecular structure and synthesis of O,O-Diisopenytl-1-benzenesulfonamido-1-trifuoromethyl-2,2,2-trifuoroethylphosphonate. *Dokl. Chem.* **345,** 296.

Clothier, B. and Johnson, M.K. (1979). Rapid aging of neurotoxic esterase after inhibition by di-isopropyl phosphorofluoridate. *Biochem. J.* **177,** 549-558.

Clothier, B. and Johnson, M.K. (1980). Reactivation and aging of neurotoxic esterase inhibited by a variety of organophosphorus esters. *Biochem. J.* **185,** 739-747.

Cygler, M., Schrag, J.D., Sussman, J.L., Harel, M., Silman, I., Gentry, M.K., and Doctor, B.P. (1993). Relationship between sequence conversion and three-dimensional structure in a large family of esterases, lipases, and related proteins. *Protein Sci.* **2,** 366-382.

Davis, C.S. and Richardson, R.J. (1980). Organophosphorus compounds, in *Experimental and Clinical Neurotoxicology* (Spencer, P.S., Schaumburg, H.H., Eds.) pp. 527-544, Williams and Wilkins, Baltimore.

Ellman, G.L., Courtney, K.D., Andres, Jr., V., and Featherstone, R.M. (1961). A new and rapid colorimetric determination of acetylcholinesterase activity. *Biochem. Pharmacol.* **7,** 88-95.

Glynn, P. (2000). Neural development and neurodegeneration: two faces of neuropathy target esterase. *Progress in Neurobiology* **61,** 61-74.

Glynn, P. (2003). NTE: one target protein for different toxic syndromes with distinct mechanisms? *BioEssays* **25,** 742-745.

Glynn, P. (2006). A mechanism for organophosphate-induced delayed neuropathy. *Toxicology Letters* **162,** 94-97.

Glynn, P., Holton, J.L., Nolan, C.C., Read, D.J., Brown, L., Hubbard, A., and Cavanagh, J.B. (1998). Neuropathy target esterase: immunolocalization to neuronal cell bodies and axons. *Neuroscience* **83,** 295-302.

Glynn, P., Read, D.J., Lush, M.J., Li, Y., Atkins, J. (1999). Molecular cloning of neuropathy target esterase (NTE) *Chem. Biol. Interact.* **119-120,** 513-517.

Hall, S.M. (1972). The effect of injections of lysophosphatidyl choline into white matter of the adult mouse spinal cord. *J. Cell Sci.* **10,** 535-546.

Holmstedt, B. (1959). Pharmacology of organophosphorus cholinesterase inhibitors. *Pharmacol. Rev.* **11,** 567-688.

Johnson, M.K. (1969). The delayed neurotoxic action of some organophosphorus compounds. Identification of the phosphorylation site as an esterase. *Biochem. J.* **114,** 711-717.

Johnson, M.K. (1970). Organophosphorus and other inhibitors of brain neurotoxic esterase and the development of delayed neurotoxicity in hens. *Biochem. J.* **120,**

523-531.

Johnson, M.K. (1977). Improved assay of neurotoxic esterase for screening organophosphates for delayed neurotoxicity potential. *Arch. Toxicol.* **37,** 113-115.

Johnson, M.K. (1982). The target for initiation of delayed neurotoxicity by organophosphorus esters: biochemical studies and toxicological applications. *Rev. Biochem. Toxicol.* **4,** 141-212.

Johnson M.K. (1990). Organophosphates and delayed neuropathy – is NTE alive and well? *Toxicol. Appl. Pharmacol*. **102,** 385–399.

Kropp, T.J. and Richardson, R.J. (2003). Relative inhibitory potencies of chlorpyrifos oxon, chlorpyrifos methyl oxon, and mipafox for acetylcholinesterase versus neuropathy target esterase. *J. Toxicol. Environ. Health A.* **12,** 1145-1157.

Kropp, T.J., and Richardson, R.J. (2006). Aging of mipafox-inhibited human acetylcholinesterase proceeds by displacement of both isopropylamine groups to yield a phosphate adduct. *Chem. Res. Toxicol.* **19,** 334-339.

Karczmar, A. (1998). Anticholinesterases: dramatic aspects of their use and misuse. *Neurochem. Int.* **32,** 401-411.

Kayyali, U.S., Moore, T.B., Randall, J.C., and Richardson, R.J. (1991). Neurotoxic esterase (NTE) assay: Optimized conditions based on detergent-induced shifts in the phenol/4-aminoantipyrine chromophore spectrum. *J. Anal. Toxicol.* **15,** 86-89.

Kretzschmar, D., Hasan, G., Sharma, S., Heisenberg, M., and Benzer, S. (1997). The swiss cheese mutant causes glial hyperwrapping and brain degeneration in *Drosophila*. *J. Neurosci.* **17,** 7425-7432.

Li, Y., Dinsdale, D., and Glynn, P. (2003). Protein domains, catalytic activity, and subcellular distribution of neuropathy target esterase in mammalian cells. *J. Biol. Chem.* **278,** 8820-8825.

Lotti, M. and Johnson, M.K. (1978). Neurotoxicity of organophosphorus pesticides: Predictions can be based on in vitro studies with hen and human enzymes. *Arch. Toxicol.* **41,** 215-221.

Lotti, M. and Moretto, A. (2005). Organophosphate-induced delayed polyneuropathy. *Toxicol Rev.* **24**, 37-49.

Lush, M.J., Li, Y., Willis, A.C., and Glynn, P. (1998). Neuropathy target esterase and a homologous *Drosophila* neurodegeneration-associated mutant protein contain a novel domain conserved from bacteria to man. *Biochem. J.* **332,** 1-4.

Makhaeva, G.F., Malygin, V.V., Aksinenko, A.Y., Sokolov, V.B., Strakhova, N.N., Rasdolsky, A.N., Richardson, R.J., and Martynov, I.V. (2005). Fluorinated α-aminophosphonates – a new type of irreversible inhibitors of serine hydrolases. *Dokl. Biochem. Biophys.* **400,** 831-835.

Moretto, A., Bertolazzi, M., Capodicasa, E., Peraica, M., Richardson, R.J., Scapellato, M.L., and Lotti, M. (1992). Phenylmethanesulfonyl fluoride elicits and intensifies the clinical expression of neuropathic insults. *Arch. Toxicol.* **66,** 67-72.

Moretto, A., and Lotti, M. (2002). The relationship between isofenphos cholinergic toxicity and the development of polyneuropathy in hens and humans. *Arch. Toxicol.* **76,** 367-375.

Moser, M., Yong, L., Vaupel, K., Kretzschmar, D., Kluge, R., Glynn, P., and Buettner, R. (2004). Placental failure and impaired vasculogenesis result in embryonic lethality for neuropathy target esterase-deficient mice. *Molec. Cell Biol.* **24,** 1667-1679.

Nauen, R., and Bretschneider, T. (2002). New modes of action of insecticides. *Pestic. Outlook* **13,** 241-245.

Ngamelue, M.N., Homma, K., Lockridge, O, and Asojo, O.A. (2007). Crystallization and X-ray structure of full-length recombinant human butyrylcholinesterase. *Acta Cryst.* **F63,** 723-727.

Nicolet, Y., Lockridge, O., Masson, P., Fontecella-Camps, J.C., and Nachon, F. (2003). Crystal structure of human butyrylcholinesterase and of its complexes with substrate and products. *J. Biol. Chem.* **42,** 41141-41147.

Pomeroy-Black M.J., Jortner, B.S., and Ehrich, M.F. (2007). Early effects of neuropathy-inducing organophosphates on in vivo concentrations of three neurotrophins. *Neurotox. Res.* **11,** 85-91.

Pope, C.N., Tanaka, D., and Padilla, S. (1993). The role of neurotoxic esterase (NTE) in the prevention and potentiation of organophosphorus-induced delayed neurotoxicity (OPIDN). *Chem. Biol. Interact.* **87**, 395-406.

Quinn, J.P., Kulakova, A.N., Cooley, N.A., and McGrath, J.W. (2007). New ways to break an old bond: the bacterial carbon-phosphorus hydrolases and their role in biochemical phosphorus cycling. *Environ. Microbiol.* **9,** 2392-2400.

Quistad, G.B., Barlow, C., Winrow, C.J., Sparks, S.E., and Casida, J.E. (2003). Evidence that mouse brain neuropathy target esterase is a lysophospholipase. *PNAS* **100,** 7983-7987.

Rainier, S., Bui, M., Mark, E., Thomas, D., Tokarz, D., Ming, L., Delaney, C., Richardson, R.J., Albers, J.W., Matsunami, N., Stevens, J., Coon, H., Leppert.,

M., and Fink, J. (2008). Neuropathy target esterase gene mutations cause motor neuron disease. *Am. J. Hum. Genet.* **82,** 780-785.

Richardson, R.J. (1995). Assessment of the neurotoxic potential of chlorpyrifos relative to other organophosphorus compounds: a critical review of the literature. *J. Toxicol. Environ. Health* **44,** 135-165.

Rosenfeld, C.A. and Sultatos, L.G. (2006). Concentration-Dependent Kinetics of acetylcholinesterase inhibition by the organophosphate paraoxon. *Toxicol. Sci.* ***90,*** *460-469.*

Russell, A.J., Berberich, J.A., Drevon, G.F., and Koepsel, R.R. (2003). Biomaterials for mediation of chemical and biological warfare agents. *Annu. Rev. Biomed. Eng.* **5,** 1-27.

Saunders, B.C. (1957). *Some aspects of chemistry and toxic action of organic compounds containing phosphorus and fluorine.* Cambridge University Press, London.

Saunders, B.C., and Stacey, G.J (1948). Esters containing phosphorus. Part IV. Di*iso*propyl fluorophosphonate. *J. Chem. Soc.* 695-699.

Sussman, J.L., Harel, M., Frolow, F., Oefner, C., Goldman, A., Toker, L., and Silman, I. (1991). Atomic structure of acetylcholinesterase from *Torpedo californica:* A prototypic acetylcholine-binding protein. *Science* **253,** 872 – 879.

Thompson, C.M. and Richardson, R.J. (2004). Anticholinesterase Insecticides. *Pesticide Toxicology and International Regulation* (T. Marrs and B. Ballantyne, Eds.) John Wiley and Sons, Ltd., Chester. pp. 89-127.

Wijeyesakere, S.J., Nasser, F.A, Kampf, J.W., Aksinenko, A.Y., Sokolav, V.B., Malygin, V.V., Makhaeva, G.F., and Richardson, R.J. (2008). Diethyl [2,2,2-trifluoro-1-phenylsulfonylamino-1-(trifluoromethyl)ethyl]phosphonate. *Acta Cryst.* **E65**, o1425-o1426.

Wijeyesakere, S.J., Richardson, R.J., and Stuckey, J.A. (2007). Modeling the tertiary structure of the patatin domain of neuropathy target esterase. *Protein J*. **26**, 165-172.

Wilson, B.W., Hooper, M., Chow, E., Higgins, R.J., and Knaak, J.P. (1984). Antidotes and neuropathic potential of isofenphos. *Bull. Environ. Contam. Toxicol.* **33,** 386 – 394.

Veronesi, B., Padilla, S., Blackmon, K., and Pope, C. (1991). A murine model of OPIDN: Neuropathic and biochemical description. *Toxicol. Appl. Pharmacol.* **107,** 311-324.

Vose, S.C., Fujioka, K., Gulevich, A.G., Lin, A.Y., Holland, N.T., Casida, J.E. (2008). Cellular function of neuropathy target esterase in lysophosphatidylcholine action. *Toxicol. Appl. Pharmacol.* **232,** 376-383.

Zaccheo, O., Dinsdale, D., Meacock, P.A., and Glynn, P. (2004). Neuropathy target esterase and its yeast homologue degrade phosphatidylcholine to glycerophosphocholine in living cells. *J. Biol. Chem.* **279,** 24024-24033.

CHAPTER 2

MASS SPECTROMETRY REVEALS THAT BUTYRYLCHOLINESTERASE IS PHOSPHORYLATED BY FLUORINATED AMINOPHOSPHONATE COMPOUNDS THROUGH A SCISSION IN THE CARBON-PHOSPHORUS BOND

Abstract

Serine esterases are inhibited by dialkyl fluorinated aminophosphonate (FAP) compounds of general formula, $(RO)_2P(O)C(CF_3)_2NHS(O)_2C_6H_5$, where R = alkyl. It has been hypothesized that the active site serine of the esterase covalently attaches to the phosphoryl moiety of the FAP compound, resulting in formation of a dialkyl phosphate adduct that can age by net loss of an R-group. However, this mechanism would require an unusual inhibition reaction involving scission of a P—C bond. The present work tested this hypothesis by using FAP compounds with R-groups of varying length and branching, and identifying adducts on treated horse serum butyrylcholinesterase using peptide mass mapping with surface-enhanced laser desorption/ionization time-of-flight mass spectrometry. Observed and predicted mass shifts were statistically identical for inhibited and protonated aged adducts, respectively. The results support the hypothesis that FAP compounds inhibit serine esterases by scission of the P—C bond, in agreement with

predictions from computational modeling and X-ray studies. Furthermore, these data support aging of the phosphoryl adduct yielding a monoalkyl phosphoryl adduct.

Introduction

The study of organophosphate toxicology is relevant today, as there are hundreds of compounds developed for use as insecticides, fungicides, lubricants, hydraulic fluids, plasticizers, flame retardants, fuel additives, pharmaceuticals, and weapons of biochemical warfare or terrorism compounds. Interactions of certain OP compounds with serine esterases are of heightened interest due to their potential use as biochemical warfare agent since the intoxication may not be detected for weeks after exposure. Over 1000 serine hydrolases have been identified in humans whose physiology is mostly unstudied (Casida and Quistad, 2005). One of these serine hydrolases, butyrylcholinesterase (BChE) is found both in the synaptic spaces of cholinergic neurons and in circulating plasma and functions to hydrolyze endogenous and exogenous choline and noncholine esters (Nicolet, *et al.* 2003). A loss of BChE function causes an increased sensitivity to cholinergic toxins; conversely by increasing circulating BChE, OP toxicity can be prevented (Broomfield *et al.,* 1991, Sparks, *et al.,* 1999).

Fluorinated aminophosphonates (FAP) (Figure 2.1) were found to inhibit serine esterases *in vitro* (Makhaeva *et al.*, 2005). These FAP compounds lack a standard electrophilic leaving group and requires that phosphorylation of the serine esterase break a carbon-phosphorus (C—P) bond, which is biochemically a stable, nonreactive bond (Quinn, *et al.* 2007). Molecular modeling and X-ray crystallography reveal that the C—P

bond in FAP compounds is made longer and weaker by the adjacent trifluoromethyl groups, supporting the hypothesis that FAP compounds inhibit serine esterase via covalent phosphylation involving a break in the C—P bond (Chekhlov, *et al.*,1995, Makhaeva *et al.,* 2005, Wijeyesakere, *et al.*, 2008). Peptide digests of horse serum butyrylcholinesterase (hsBChE) were used to calculate the bimolecular rate of inhibition with the FAP compounds and compare masses of the unadducted and adducted active site peptides to reveal if the FAP compounds phosphorylate serine esterases through a break in the C—P bond, and subsequently age through net loss of an alkyl group.

Materials and Methods

Materials

Lyophilized hsBChE, was purchased from Sigma-Aldrich (St. Louis, MO), diluted in 50 mM ammonium bicarbonate buffer pH 8.0, and stored at −80°C. Porcine trypsin was purchased from Sigma-Aldrich (St. Louis, MO), diluted in 1 mM HCl, and stored at −80°C. Butyrylthiocholine (BTCh) and 5,5′-dithio-bis(2-nitrobenzoic acid) (DTNB) were purchased from Sigma-Aldrich (St. Louis, MO). The fluorinated aminophosphonate (FAP) compounds were synthesized by the Institute for Physiologically Active Compounds, Chernogolovka, Russia, and identified by NMR (Makhaeva, 2005). These include (1-Benzenesulfonylamino-2,2,2-trifluoro-1-trifluoromethyl-ethyl)-phosphonic acid dimethyl ester (methyl-FAP), diethyl ester (ethyl-FAP), diisopropyl ester (isopropyl-FAP), dipropyl ester (*n*-propyl-FAP), diisobutyl ester (isobutyl-FAP), di*sec*-butyl ester (*sec*-butyl-FAP),), dibutyl ester (*n*-butyl-FAP),

diisopentyl ester (isopentyl-FAP), dipentyl ester (*n*-pentyl-FAP), and dihexyl ester (*n*-hexyl-FAP). All FAP compounds were appropriately contained within a fume hood, and any instruments or containers used in the process were soaked in > 1M NaOH to inactivate the compounds before disposal because of suspected cholinergic and neuropathic effects (Doorn *et al.,* 2000, Kropp *et al.,* 2007).

Measurement of Cholinesterase Activity and Inhibition

Activity of hsBChE was determined colorimetrically in 0.1 M sodium phosphate buffer pH 7.8, and carried out at 37 °C using a modification of the method of Ellman *et al.* (1961). Inhibitors were diluted in dimethyl sulfoxide (DMSO) or acetone with a final solvent concentration ≤ 1 % (v/v), which has been shown not to affect enzyme activity significantly (data not shown). Enzyme and inhibitor were incubated for several measured time points up to 12 minutes. The prewarmed substrate solution containing BTCh (1.0 mM final concentration) and DTNB (0.32 mM final concentration) was then added to the enzyme mixture. The residual activity of the hsBChE was determined by measuring the change in absorbance at 412 nm over a 20-min period at 37 °C using a SPECTRAmax 340 microplate reader (Molecular Devices Corp., Sunnyvale, CA).

Calculation of k_i

The apparent bimolecular rate constants of inhibition (k_i) of the FAP compounds against hsBChE was determined as previously described for OP interactions with serine esterases (Aldridge and Reiner, 1972, Jianmongkol *et al.*, 1999, Kropp and Richardson, 2003). The reaction with FAP was carried out so that the concentration of the inhibitor

([*I*]) > 10 *x* [BChE] and [*I*] << K_d. These conditions were used so that k_i could be measured using linear regression to model pseudo-first-order kinetics. The slopes of the primary linear kinetic plots of ln(% activity) vs time (*t*) are the apparent first-order rate constants of inhibition (*k'*) for each [*I*]. The slope of the secondary linear kinetic plot of –*k'* vs [*I*] is the k_i for the inhibitor. For each experiment four time points and at least five inhibitor concentrations in duplicate were used, and three separate experiments were performed for statistical analysis. Plots and regressions were carried out using Prism version 4.0 for Windows, GraphPad Software, Inc. (San Diego, CA).

Mass Spectrometry

5 μg hsBChE was incubated with each FAP compound at an appropriate concentration and time to produce ~90% inhibited OP-enzyme complex, which was calculated by using the equation $I_{90} = \ln(10)/(k_i \times t)$. Samples from each time point were coupled with a control, which was diluted to an equivalent concentration of solvent and buffer. This mixture was diluted 1:20 – 1:50, stored at room temperature for 0 – 72 hours, then digested with 50 ng trypsin for 3 – 16 h at 37 °C. 1 μL of each sample was then placed on an H4 (hydrophobic surface) chip (Ciphergen Biosystems, Inc, Fremont, CA), and allowed to dry at room temperature. Lastly, 1 μL of α-cyano-4-hydroxycinnamic acid (CHCA) matrix solution consisting of a 1:1 (v/v) solution of acetonitrile (ACN) and 1% (w/v) trifluoroacetic acid (TFA) consisting of a 20% (v/v) was placed on top of each spot and allowed to dry at room temperature. A PBS-IIc surface-enhanced laser desorption/ionization time-of-flight mass spectrometer (SELDI-TOF MS) (Ciphergen Biosystems, Inc) equipped with a nitrogen laser (337 nm, 4 ns pulse width) was used to

acquire spectra. An acceleration voltage of 20 kV was used, and 150-200 laser shots were averaged for each spectrum. The sequence of hsBChE was acquired from the NCBInr database (NP 001075319). Each spectrum was internally calibrated by digestion peptides 437-452 (2043.21 Da), 248-268 (2222.72 Da), 134-159 (2764.15 Da), and 176-208 (3544.09 Da). The expected average *m/z* values for the singly charged unit (MH^+) corresponding to the internal calibration peptides and the active site peptide RSVTLFGESAGAASVSLHLLSPRS containing the active serine (underlined) from tryptic digests of hsBChE were obtained from ProteinProspector version 5.1.4 (http://prospector.ucsf.edu). Values for predicted adducts were calculated by subtracting the proton lost by phosphorylation of the active site serine, and adding the masses of the phophorylation product, either intact, or aged by the loss of a singly alkyl. The experimental values were compared to the predicted values using a one-sample t-test.

Results

To ensure that FAP compounds were not added in excess and would not interfere with the serine containing trypsin, k_i values were determined and shown in Table 2.1. These data were used to calculate 90% inhibition (I_{90}) at 10-30 min (see Methods). Kinetic values of aging were not calculated, because the rate of aging of a particular alkyl group should be consistently independent of the rate of inhibition. Furthermore, previously reported half-lives ($t_{1/2}$) of aging of methyl esters were 3.9 hours (Worek *et al.,* 1999), ethyl esters between 12.6 and 7.2 hours (Mason *et al*., 1993, Masson *et al.,* 1997b, Li*, et al.,*2007), isopropanol esters were close to 1 hour (Masson *et al.,* 1997a,

Kropp and Richardson, 2007), cyclohexyl esters were 2.2 hours (Worek *et al.,* 1998, Bartling *et al.,* 2007), and pinacolyl esters were between 9 minutes and 3.9 minutes (Saxena *et al.,* 1998, Masson *et al*., 1997a), and agreeable across human and equine species (Kropp and Richardson, 2007). Aging was allowed to proceed for up to 72 h before tryptic digestion, to ensure the collection of at least three spectra containing an inhibited adduct and three spectra containing an aged adduct. If the FAP compound does indeed inhibit the BChE in the expected manner, then the moieties of the covalently bound phosphorylated and aged adducts on the active site serine will be as shown in Figure 2.2. Indeed, the spectra for each FAP analogue showed a reduction of the active site peptide peak, and an appearance of 1-2 peaks that corresponded to a predicted inhibited and/or aged phosphoryl adduct.

In the unadducted hsBChE spectrum, the active site peptide peak is identified at 2201.39 *m/z*, and there is an absence of identifiable peaks between 2300 – 2500 *m/z* (Figure 2.3). In each of the FAP-BChE spectra, there is a reduction in the active site peptide peak, and an emergence of peaks in the identified range, which correspond to phosphoryl adducts. The average peptide map coverage for the treated and the untreated spectra were 66%, which includes BChE peptides, and trypsin auto-digest peptides. When these peaks were analyzed by peptide mass fingerprint program found in mascot (www.matrixscience.com) with a tolerance of ±1 Da, hsBChE was identified. Table 2.2 compares the mass shifts observed in each spectra with corresponding predicted adduct size. The predicted and observed masses for the inhibited FAP-BChE adducts were statistically equivalent. The observed peaks corresponding to aged active site peptide adducts were significantly larger than the predicted adduct size by one dalton.

Interestingly, these values were statistically identical to a protonated adduct. A peak corresponding to an inhibited *n*-hexyl-FAP adduct was not observed; however, a peak corresponding to the protonated aged peak was observed. A peak corresponding to an aged isobutyl-FAP adduct was not observed, even after 72 h, although a peak corresponding to an inhibited adduct was observed.

Discussion

The unidentifiable peaks may be due to glycosylated peptides, since the protein was not treated with a glycosylase and hsBChE is known to be glycosylated (Saxena *et al.*, 1997). These peaks were found in both control and FAP treated samples, and did not impede analysis of the mass shifts. Predicted and theoretical mass shifts of peaks corresponding to a given dialkyl phosphoryl adduct were statistically identical to each other, indicating that the FAP compounds phosphorylate the active site serine of BChE as shown in Figure 2.2. The predicted masses of the peaks corresponding to aged adducts were one amu lower than the respective observed masses, but each of these values were statistically equivalent to the respective masses protonated adducts. Because the matrix applied to crystallize the protein before SELDI-TOF MS analysis is an acidic solution of TFA and CHCA, which the negatively charged oxygen left after the dealkylated aged phosphoryl group would be expected to be protonated.

There was no aged adduct observed in isobutyl-FAP adducted hsBChE; however, the absence of the aging of an isobutyl alkyl group was also observed in the methyl, isobutyl-ester substituted thiophosphonate Russian-VX, (VR)-inhibited BChE (Li *et al.*,

2007). This could be because the arrangement of the alkyl chain within the binding site pocket may sterically hinder the aging process. The methyl, isobutyl-ester analogue of sarin was found to have a $t_{1/2}$ for aging of 43 for BChE respectively, but there was no MS analysis to prove the aged phosphoryl adduct was indeed responsible for the absence of reactivation (Bartling, *et al.,* 2007). There was also an absence of an *n*-hexyl FAP-BChE inhibited adduct. This would indicate that the *n*-hexyl FAP-BChE complex is completely aged at three hours. As stated previously, the reported $t_{1/2}$ for aging of other hexyl branched moieties including cyclohexyl and the pinocolyl both age within two hours, and no data could be found regarding the aging of *n*-hexyl esters with BChE. Previous reports have found that branched alkyl groups age faster in phosphonylated BChE than the straight alkyl phosphoryl moieties, however this was determined using only the propyl and butyl alkyl esters (Bartling, *et al.,* 2007).

In conclusion, the observed mass shifts of the active site peptide peak support the hypothesis that hsBChE is inhibited by the FAP compounds through scission of the C—P bond, which leads to covalent phosphorylation. This contention is further supported by the appearance of peaks corresponding to net loss of an alkyl group from the BChE-dialkylphosphoryl conjugate, indicating that aging occurs in the expected manner.

Table 2.1. Bimolecular rates of inhibition (k_i) for FAP compounds

Compound	k_i ($M^{-1}min^{-1}$)
methyl - FAP	$4.65 \pm 0.08 \times 10^2$
ethyl - FAP	$1.02 \pm 0.04 \times 10^5$
isopropyl - FAP	$1.21 \pm 0.08 \times 10^4$
***n*-propyl - FAP**	$5.20 \pm 0.06 \times 10^5$
***sec*-butyl - FAP**	$1.75 \pm 0.16 \times 10^4$
isobutyl - FAP	$1.89 \pm 0.06 \times 10^5$
***n*-butyl - FAP**	$7.09 \pm 0.32 \times 10^5$
isopentyl - FAP	$5.57 \pm 0.80 \times 10^5$
***n*-pentyl - FAP**	$5.60 \pm 0.76 \times 10^5$
***n*-hexyl -FAP**	$7.37 \pm 0.57 \times 10^5$

Data calculated as mean ± SEM, $n = 3$

Table 2.2. Theoretical and calculated mass shifts of inhibited and aged adducted serine peptides.

		Predicted	Observed
methyl	inhibited	108.0	108.1 ± 0.3
	aged	93.0	93.9 ± 0.1
ethyl	inhibited	136.1	136.1 ± 0.1
	aged	107.0	108.0 ± 0.1
***n*-propyl**	inhibited	164.2	164.2 ± 0.1
	aged	121.1	122.2 ± 0.0
isopropyl	inhibited	164.2	164.1 ± 0.1
	aged	121.1	121.9 ± 0.2
***n*-butyl**	inhibited	192.2	192.4 ± 0.2
	aged	135.1	136.0 ± 0.2
isobutyl	inhibited	192.2	192.1 ± 0.1
	aged	135.1	*n.o.*
***sec*-butyl**	inhibited	192.2	192.8 ± 0.4
	aged	135.1	136.5 ± 0.3
***n*-pentyl**	inhibited	220.3	220.1 ± 0.1
	aged	149.1	150.2 ± 0.1
isopentyl	inhibited	220.3	220.1 ± 0.5
	aged	149.1	150.1 ± 0.1
***n*-hexyl**	inhibited	248.3	*n.o.*
	aged	163.1	164.1 ± 0.2

n.o. – peaks were not observed. Data calculated as mean ± SEM, $n \geq 3$

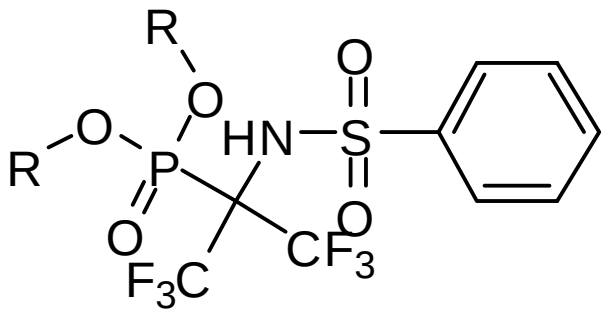

Figure 2.1. General structure of FAP compounds. The alkyl groups vary in length and branching, where R= methyl, ethyl, *n*-propyl, isopropyl, *n*-butyl, isobutyl, *sec*-butyl, *n*-pentyl, isopentyl, and *n*-hexyl.

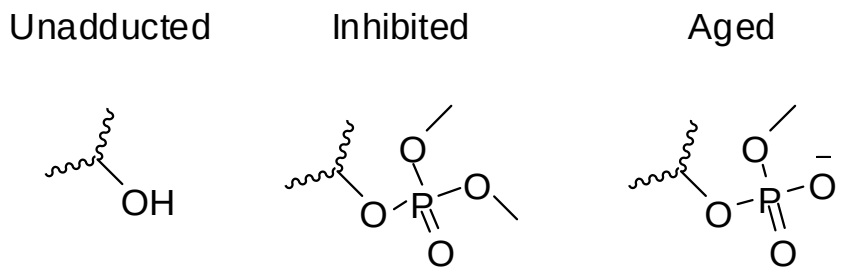

Figure 2.2. Scheme of unadducted, FAP-inhibited, and FAP-aged serine. The unadducted active site serine of hsBChE is found at 2201.39 *m/z.* If the FAP compounds phosphorylate the serine, and subsequently age, the mass of these adducts can be predicted by subtracting the loss of the serine proton, and adding the phophorylated product.

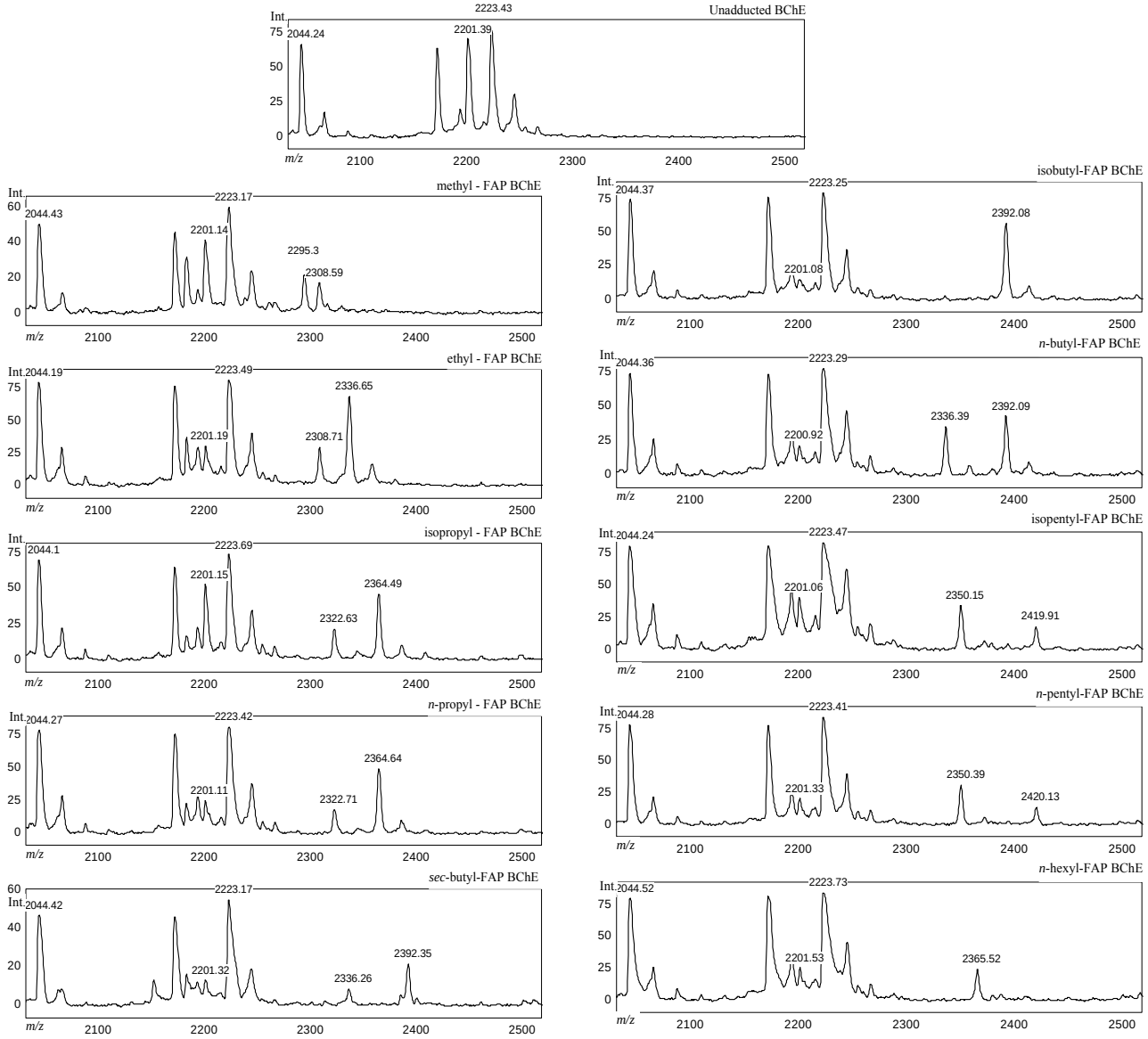

Figure 2.3. Representative spectra for tryptic digests of unadducted hsBChE (top) and FAP-adducted hsBChE. The peaks at ~2044 and ~2224 *m/z* correspond to internal calibration peptides 437-452 and 248-268 respectively. In the unadducted hsBChE spectrum, the peak at 2201.39 *m/z* corresponds to the peptide containing the active site serine. Subsequent spectra show emergent peaks appearing at mass shifts corresponding to inhibited and aged active site peptide adducts.

References

Aldridge, W.N., and Reiner, E. (1972). *Enzyme Inhibitors as Substrates: Interactions of Esterases with Esters of Organophosphorus and Carbamic Acids.* North-Holland Publishing, Amsterdam.

Bartling, A., Worek, F., Szinicz, L., and Thiermann, H. (2007). Enzyme-kinetic investigation of different sarin analogues reacting with human acetylcholinesterase and butyrylcholinesterase. *Toxicology* **233,** 166-172.

Broomfield, C.A., Maxwell, D.M., Solana, R.P., Castro, C.A., Finger, A.V., and Lenz, D.E. (1991). Protection by butyrylcholinesterase against organophosphorus poisoning in nonhuman primates. *J. Pharmacol. Exp. Ther.* **259,** 633-638.

Casida , J.E. and Quistad, G.B. (2005). Serine hydrolase targets of organophosphorus toxicants. *Chem.-Biol. Int.* **157-158,** 277-283.

Chekhlov, A.N., Aksinenko, A.Y., Sokolov, V.B., and Martynov, I.V. (1995). Crystal and molecular structure and synthesis of O,O-Diisopenytl-1-benzenesulfonamido-1-trifuoromethyl-2,2,2-trifuoroethylphosphonate. *Dokl. Chem.* **345,** 296.

Doorn, J.A., Gage, D.A., Schall, M., Talley, T.T., Thomson, C.M., and Richardson, R.J. (2000). Inhibition of acetylcholinesterase by (1*S*,3*S*)-isomalathion proceeds with loss of thiomethyl: kinetic and mass spectal evidence for an unexpected primary leaving group. *Chem. Res. Toxicol.* **13,** 1313-1320.

Ellman, G.L., Courtney, K.D., Andres, Jr., V., and Featherstone, R.M. (1961). A new and rapid colorimetric determination of acetylcholinesterase activity. *Biochem. Pharmacol.* **7**, 88-95.

Jianmongkol, S., Marable, B.R., Berkman, C.E., Tally, T.T, Thompson, C.M., and Richardson, R.J. (1999). Kinetic evidence for different mechanisms of acetylcholinesterase inhibition by (1*R*)- and (1*S*)-stereoisomers of isomalathion. *Toxicol. Appl. Pharmacol.* **155** 43-53.

Kropp, T.J. and Richardson, R.J. (2003). Relative inhibitory potencies of chloryrifos oxon, chlorpyrifos methyl oxon and mipafox for acetylcholinesterase versus neuropathy target esterase. *J. Toxicol. Environ. Health A* **66,** 1145-1157.

Kropp, T.J. and Richardson, R.J. (2007). Mechanism of aging of mipafox-inhibited butyrylcholinesterase. *Chem. Res. Toxicol.* **20,** 504-510.

Li, H., Schopfer, L.M., Nachon, F., Froment, M.-T., Masson, P., Lockridge, O. (2007). Aging pathways for organophosphate-inhibited human butyrylcholinesterase, including novel pathways for isomalathion resolved by mass spectrometry. *Toxicol. Sci.* **100**, 136-145.

Makhaeva, G.F., Malygin, V.V., Aksinenko, A.Y., Sokolov, V.B., Strakhova, N.N., Rasdolsky, A.N., Richardson, R.J., and Martynov, I.V. (2005). Fluorinated α-aminophosphonates – a new type of irreversible inhibitors of serine hydrolases. *Dokl. Biochem. Biophys.* **400**, 831-835.

Mason, H.J., Waine,E.,Stevenson,A.,and Wilson,H.K. (1993). Aging and spontaneous reactivationof human plasma cholinesterase activity after inhibition by organophosphorus pesticides. *Hum. Exp. Toxicol.* **12,** 497-503.

Masson, P., Fortier, P.L., Albaret, C., Froment, M.T., Bartels, C.F., and Lockridge,O. (1997a). Aging of di-isopropyl-phosphorylated human butyrylcholinesterase. *Biochem J.* **327,** 601-607.

Masson, P., Froment, M.T., Bartels, C.F., and Lockridge, O. (1997b). Importance of aspartate-70 in organophosphate inhibition, oxime reactivation and aging of human butyrylcholinesterase. *Biochem. J.* **325,** 53-61

Nicolet, Y., Lockridge, O., Masson, P., Fontecilla-Camps, J.C., and Nachon, F. (2003). Crystal structure of human butyrylcholinesterase and of its complexes with substrate and products. *J. Biol. Chem.* **276,** 41141-41147.

Quinn, J.P., Kulakova, A.N., Cooley, N.A., and McGrath, J.W. (2007). New ways to break an old bond: the bacterial carbon-phosphorus hydrolases and their role in biochemical phosphorus cycling. *Environ. Microbiol.* **9,** 2392-2400.

Saxena, A., Raveli, L., Ashani, Y., and Doctor, B.P. (1997). Structure of glycan moieties responsible for the extended circulatory life time of fetal bovine serum acetylcholinesterases and equine serum butyrylcholinesterase. *Biochemistry* **36,** 7481-7489.

Saxena, A.,Viragh, C., Frazier, D.S., Kovach, I.M., Maxwell, D.M., Lockridge, O. and Doctor, B.P. (1998). The pH dependence of dealkylationin soman-inhibited cholinesterases and their mutants: further evidence for a push-pull mechanism. *Biochemistry* **39,** 15086-15096.

Sparks, S.E., Quistad, G.B., and Casida, J.E. (1999). Organophosphours pesticide-induced butyrylcholinesterase inhibition and potentiation of succinylcholine toxicity in mice. *J. Biochem. Mol. Toxicol.* **13,** 113-118.

Wijeyesakere, S.J., Nasser, F.A., Kampf, J.W., Aksinenko, A.Y., Sokolov, V.B., Malygin, V.V., Makhaeva, G.F., and Richardson, R.J. (2008). Diethyl [2,2,2-trifluoro-1-phenyl-sulfonylamino-1-(trifluoromethyl)-ethyl]phosphonate. *Acta Cryst.* **E64**, o1425.

Worek, F., Diepold, C., and Eyer, P. (1999). Dimethylphosphoryl-inhibited human cholinesterasese: inhibition, reactivation, and aging kinetics. *Arch.Toxicol.* **73,** 7-14.

Worek, F., Eyer, P., and Szinicz, L. (1998). Inhibition, reactivation and aging kinetics of cyclohexylmethylphosphonofluoridate inhibited human cholinesterases. *Arch. Toxicol.* **72,** 580-587.

CHAPTER 3

ASSESSMENT OF DELAYED NEUROTOXICITY POTENTIAL OF ORGANOPHOSPHORUS COMPOUNDS *IN VITRO*

Abstract

Organophosphorus (OP) compounds covalently phosphylate serine hydrolases, thus inhibiting their function. When this occurs in neuropathy target esterase (NTE), followed by an aging process, a latent and distal axonal degeneration occurs, and this is described as OP induced delayed neuropathy (OPIDN). If an OP compound is a substantially more potent inhibitor of acetylcholinesterase (AChE) than of NTE, then cholinergic toxicity could result in lethality, thus obviating the development of OPIDN. However, if the OP compound is neuropathic, cholinergic toxicity will be mild, and sufficient NTE will be inhibited and aged to initiate OPIDN. The current standard animal model of OPIDN is the hen, but due to the size and cost of animal husbandry, this is a burdensome model for testing OP compounds for their neuropathic potential. The present research was carried out in order to develop an *in vitro* protocol based on correlations in the catalytic properties of hen brain NTE and AChE with human recombinant and mouse brain enzymes. These data show that all three enzyme systems provide suitable methods for *in vitro* testing to predict inhibitory kinetics and relative inhibitory potential, thereby affording an initial screen of neuropathic potential of OP compounds.

Introduction

This protocol was developed as a screening tool to assess *in vitro* the neuropathic potential of organophosphorus (OP) compounds, i.e., their ability to produce OP compound-induced delayed neurotoxicity (OPIDN). This syndrome involves distal sensorimotor degeneration of long large-diameter axons in spinal cord and peripheral nerves with associated sensory deficits and paralysis occurring within 1–4 weeks after exposure (Richardson, 2005). Mechanistic research indicates that inhibition and aging of > 70% of neuropathy target esterase (NTE) in neural tissue initiates OPIDN and that inactivation of acetylcholinesterase (AChE) is not involved. Studies with enzymes from hen and human brain have shown that the neuropathic potential of an OP compound can be assessed by its relative inhibitory potency (RIP) against AChE vs NTE. A high RIP value indicates that the compound will produce cholinergic toxicity rather than OPIDN. The current work extends previous results to enzymes from mouse brain as well as recombinant human enzymes (AChE and NTE esterase domain, NEST).

Inhibition of NTE consists of phosphylation of its active site serine, and aging involves net loss of a side chain from the phosphyl moiety yielding a negatively charged OP-NTE conjugate that is intractable to reactivation. Inhibition and aging can occur within minutes of dosing; therefore, these events do not constitute the rate-limiting steps in the development of OPIDN (Richardson, 2005). Apart from the inhibition and aging of NTE, there is a large gap in understanding concerning the events that transpire between exposure to a neuropathic OP compound and the emergence of OPIDN. Elucidation of

the pathophysiology and mechanism of OPIDN, as well as the assessment of OP compounds for their neuropathic potential, have been hampered by a lack of knowledge concerning the physiological function of NTE and deficiencies in available models, either *in vivo* or *in vitro* (Pomeroy-Black *et al.*, 2007). Thus, it has been difficult to develop models that accommodate such features as the apparent need for axons of sufficient length and caliber, differences in cholinergic and neuropathic thresholds *in vivo*, species differences in biotransformation of OP toxicants and protoxicants, and higher susceptibility of adult versus young animals (Moretto and Lotti, 2002).

Currently, the most widely accepted *in vivo* model for the study of OPIDN or assessment of the neuropathic potential of OP compounds is the adult hen. Test compounds are administered to hens, and brain NTE inhibition is measured in a cohort of animals at a specified time, usually 24–72 hours after dosing. Another cohort of dosed animals is followed for 28 days and assessed for clinical signs of OPIDN; following sacrifice, animals are processed for histopathological examination of axonal lesions in spinal cord and peripheral nerves (USEPA, 1998). However, compared to the usual laboratory rodents (e.g., rats or mice), hens are difficult to acquire and maintain for laboratory studies, and their substantially larger size requires considerably greater amounts of test materials for dosing *in vivo*. Consequently, it would be of interest to develop a rodent model for studying at least some aspects of OPIDN and/or for assessing the neuropathic potential of OP compounds.

Rats have been thought to be resistant to OPIDN, because they do not readily display clinical signs of hind limb paralysis, despite exposure to high levels of neuropathic compounds (Abou-Donia, 1981). Mice have been considered to be even less

suitable than rats, because of the difficulty in achieving > 70% inhibition of NTE *in vivo* following dosing with neuropathic OP compounds (Veronesi *et al.,* 1991). The relative intractability of rodents to OPIDN has been attributed to a variety of potential factors, including rates of aging and resynthesis of NTE, axonal length, repair of axonal lesions, and chronological age (most rat studies have used animals under 3 months of age, whereas most hen studies have been carried out with animals at least 8 months of age). Nevertheless, rodents possess brain AChE and NTE activity, and the present work demonstrates that inhibition *in vitro* of these esterases from mouse brain can be used as a suitable predictor of neuropathic potential of OP compounds. Furthermore, it is recommended that AChE and NTE inhibition *ex vivo* could be used in mice in order to incorporate the factors of absorption, distribution, metabolism, and excretion (ADME) into the predictive model.

Experimental Protocol

Suppliers

Suppliers or manufacturers for materials are indicated within each procedure. Standard reagents are reagent grade or the highest grade commercially available purchased from typical suppliers, e.g., Sigma or Fisher.

Preparation of Brain Tissue

Adult white leghorn hens (Dr. Steve Bursian, Department of Animal Science, Michigan State University, E. Lansing, MI) and adult male and/or female C57/bl mice (Dr. Shirley Rainier, Department of Neurology, University of Michigan, Ann Arbor, MI)

were euthanized via CO_2 asphyxiation. Brains were immediately removed, weighed, and placed on dry ice for transport; they were stored at −80 °C until use, usually within 24 hr. The brains were thawed and homogenized in 0.32 M sucrose (~10% w/v) at 4 °C. The homogenates were then centrifuged 9000 × *g* for 20 min at 4 °C. Aliquots of the supernatants (brain S9 fraction) were stored at −80 °C until use.

Production and Purification of Human Recombinant NEST

Because full-length NTE is difficult to isolate or produce, human recombinant NTE esterase domain (NEST) was used as a surrogate for studies *in vitro* that require pure and/or human protein rather than a tissue preparation containing NTE activity. NEST contains residues 727-1,216 of NTE and includes the active site serine. It is the shortest segment of NTE that retains esterase activity; moreover, the catalytic properties of NEST, including the response to OP inhibitors, closely resemble those of full-length NTE (Atkins and Glynn, 2000; Atkins *et al*., 2002; Kropp *et al*., 2004; Van Tienhoven *et al*., 2002). The procedure for production and purification of NEST were modified from Atkins and Glynn (2000) and Atkins *et al*. (2002), as described below.

Transformation for plasmid and protein expression

Competent DH5α *E. coli* cells were stored at −80 °C until use. They were then placed in an ice bath to thaw. Once thawed, a 50 μL aliquot was placed into a microfuge tube prechilled to 4 °C. DNA plasmid encoding NEST with a C-terminal His_6-tag (Dr. Paul Glynn, MRC Toxicology Unit, Leicester, UK) was added to the cells. They were then swirled to mix and incubated at 4 °C for 30 min. This step allowed the plasmid to

attach itself to the outside of the cell membrane. The mixture was heat-shocked for 90 sec at 42 °C to open the pores within the membrane and allow the plasmids to enter the cells. The heat-shocked cells were then returned to the ice bath for 2 min to close and seal the pores. Preheated NZY^+ (an enriched broth containing casein hydrolysate (NZ) amine, yeast extract, NaCl, $MgCl_2$, $MgSO_4$, and glucose), LB (media that contains NaCl, tryptone, and yeast extract) containing 0.1 μM of the antibiotic ampicillin was added, and the mixture was incubated at 37 °C for 1 hr with shaking. This mixture was then centrifuged on a table-top centrifuge at 12,000 × *g* for 2 min. A 400 μL aliquot of the supernatant was removed and the pellet was resuspended in the remaining supernatant. The suspension was then placed on an agar plate containing ampicillin and placed overnight into a 37 °C incubator. Once colonies were formed, one was chosen for an overnight incubation in 10 mL NZY^+ LB media containing 0.1 μM ampicillin at 37 °C for DNA isolation. The plated colonies were then stored at 4 °C for up to 30 days.

DNA isolation

The plasmids were purified using the QIAprep kit from QIAGEN. The overnight culture was transferred to a sterile 15 mL centrifuge tube and centrifuged at 700 × *g* for 20 min at 4 °C. The pellet was resuspended in 250 μL of kit buffer labeled P1 with RNase. This suspension was transferred to a microfuge tube. To digest the RNA without shearing the DNA, 250 μL of kit buffer labeled P2 was added; the mixture was immediately inverted 4–6 times and allowed to stand for no more than 5 min. Kit buffer labeled P3 was added; the tube was immediately inverted 4–6 times and centrifuged on a table-top centrifuge at 12,000 × *g*. The supernatants were then placed into the spin

column provided in the kit and centrifuged for 1 min at 12,000 × *g*; the flow-through was discarded. The column was washed with 750 μL of PE buffer provided in the kit, incubated for 1 min, and centrifuged at 12,000 × *g* for 1 min; the flow-through was discarded. The spin column was placed into a clean tube, and the DNA was eluted with 50 μL of kit EB buffer, allowed to stand for one minute, and then centrifuged for 1 min at 12,000 × *g*. The flow-through was stored at –20 °C until use, and the DNA sequence was verified (e.g., using the DNA Core at the Life Sciences Institute in the University of Michigan).

Protein expression

A culture was chosen at random from the agar plate for the *E. coli* strain and cultured overnight in "terrific broth" media (containing tryptone, yeast extract, and glycerol, and buffered with potassium phosphate) containing 0.1 μM ampicillin. The cultures were diluted 1:100–1:1000 (such that the $OD_{600} < 0.1$) and grown at 37 °C for 1–3 hours, until the $OD_{600} \approx 1.0$. The temperature was reduced to 20 °C for 1 hr, and then the cells were induced with 0.4 mM isopropyl-β-D-thiogalactopyranoside (IPTG), for at least 16 hr (overnight). The cells were centrifuged for 12 min at 12,000 × g at 4 °C and the pellets were stored at –80 °C for at least 1 day, and no more than 6 months, until used for purification.

Protein purification

Cell pellets (0.5 L) were thawed on ice for 60–90 min and resuspended in 50 mL PEN buffer (50 mM sodium phosphate buffer, 300 mM NaCl, 0.1 mM EDTA, pH 8.0)

containing 3% (w/v) of the detergent, 3-[(3-cholamidopropyl)dimethylammonio]-1-propanesulfonate (CHAPS), and sonicated at 30 sec intervals for 5 min with an output of 25 mA. The resulting mixture was centrifuged at 20,000 × *g* for 60 min at 4 °C. The supernatant was absorbed onto 4 mL nickel-nitrilotriacetic acid-agarose and washed 6 times with 50 mL PEN buffer containing 0.3% (w/v) CHAPS and 10 mM imidazole. The protein was eluted with 8 mL PEN buffer containing 0.3% (w/v) CHAPS and 300 mM imidazole. The protein was then diluted to 0.1 mg/mL and mixed 1:3 – 1:4 (w/w) with 1,2-dioleoyl-*sn*-glycero-3-phosphocholine (DOPC) (Avanti) in 10% (w/v) CHAPS to make NEST-DOPC liposomes. The liposome suspensions were dialyzed (4 °C) 3 times (2 hr, 2 hr, and overnight) against 100 volumes of PEN buffer containing 1 mM dithiothreitol, using 10 kMW SnakeSkin dialysis tubing (Pierce). The fractions containing NEST were checked for MW and purity on 4-20% (w/v) Bis-Tris SDS-PAGE precast gel from Invitrogen. The apparent MW of NEST on SDS-PAGE is about 55 kDa (Atkins and Glynn, 2000).

Measurement of AChE Activity and Inhibition

AChE from hen brain (hbAChE), mouse brain (mbAChE), or the human recombinant enzyme (hrAChE) was inhibited by preincubation with OP compounds, and its residual activity was determined by a modification of the colorimetric method of Ellman *et al*. (1961) as applied in earlier studies from our laboratory (Doorn *et al*., 2003; Kropp and Richardson, 2003, 2006; Jianmongkol *et al*., 1996; Malygin *et al*., 2003). Inhibitors were diluted in water-miscible organic solvents (e.g., acetone) at a final concentration ≤ 1% (v/v), a solvent concentration range that has been previously shown

not significantly to affect enzyme activity. Serial dilutions of inhibitors were made in 50 mM Tris-Citrate buffer pH 6.0 at 25°C. Enzyme preparations were diluted in 0.1M sodium phosphate buffer pH 8.0. Enzyme and inhibitor were preincubated at 37 °C for various measured times, e.g., 0, 3, 6, 9, and 12 min. The prewarmed substrate solution contains 1.25 mM acetylthiocholine (ATCh), and 0.4 mM 5,5′-dithio-bis(2-nitrobenzoic acid) (DTNB). Substrate solution (200 μL) was added to 50 μL of the enzyme mixture in 96-well plates at the end of each preincubation interval, and the activity of AChE at 37 °C was measured by the rate at which AChE hydrolyzes ATCh to thiocholine, which then reacts with DTNB to create the yellow anion of cleaved DTNB. The chromophore could be detected and quantified by measuring the change in absorbance at 412 nm over an incubation period, e.g., 20 min, using a SpectraMax 340 microplate reader.

Measurement of AChE Aging

Inhibition and aging were carried out similarly as described in earlier studies from our laboratory (Jianmongkol *et al*., 1999; Kropp and Richardson, 2006). Aliquots of AChE were diluted using the same conditions as described in the section above on measurement of AChE activity and inhibition. The aliquots were inhibited at a sufficient concentration for 10 min with OP inhibitors to obtain ≥ 90% inhibition at 37 °C. The enzyme was then diluted 1:100 (v/v) with phosphate buffer at 25 °C, to stop inhibition. The inhibited AChE was then incubated at 25 °C for measured intervals between 0 and 48 hr. At the end of each time interval, the enzyme solution was incubated with 200 μM 2-pralidoxime methiodide (2-PAM) (1:1 v/v) for 20 min. This was done so that the measurement will truly be that of aged enzyme and not inhibited-unaged enzyme,

because 2-PAM will regenerate the AChE activity of the inhibited-unaged enzyme, but not that of the aged enzyme. Residual activity was measured as described above, at 25 °C.

Measurement of NTE/NEST Activity and Inhibition

The activity of NTE from hen brain (hbNTE) or mouse brain (mbNTE) was determined by a modification of a colorimetric assay (Kayyali *et al*., 1991), which is the phenyl valerate hydrolase activity inhibited by diethyl 4-nitrophenyl phosphate (paraoxon) but not abolished by *N*,*N*′-disopropylphosphorodiamidic fluoride (mipafox, MIP). The activity of the human recombinant esterase domain of NTE (NEST) was determined in the absence of these inhibitors (Kropp *et al*., 2004). All reactions were carried out at 37 °C for the entire assay. Homogenates were diluted in 50 mM Tris-HCl, 0.1 mM EDTA, pH 8.0 at 37 °C. The solution containing NTE was incubated with 40 μM paraoxon (final concentration) to inhibit background esterase activity, and 40 μM paraoxon and 50 μM mipafox (final concentrations) to completely inhibit NTE activity. The difference between these two activities is the operational definition of NTE activity, as stated previously. Substrate solution (100 μL) of 5.3 mM phenyl valerate/*N*,*N*'-dimethylformamide (PV/DMF) diluted in 0.03% (w/v) Triton X-100 was added, and the reaction was allowed to proceed for 20 min, during which PV was hydrolyzed by active NTE or NEST to produce phenol. Stop solution (100 μL) of 5.0 mg/mL sodium dodecyl sulfate (SDS)/1.23 mM 4-aminoantipurine (4-AAP) was added, and the reaction of 4-AAP with the phenol produced was allowed to proceed for 3 min. The chromophore was produced by adding 50 μL of a solution of 12.1 mM $K_3Fe(CN)_6$, and color was allowed

to develop and stabilize for 10 min. The endpoint absorbance was measured at 486 nm using a SpectraMax 340 microplate reader. Test inhibitors were prepared and diluted as described in the section above on measurement of AChE activity and inhibition. For NTE, test inhibitors were added at the end of the first preincubation interval and inhibition was continued for various measured times, usually between 0 and 20 min, before addition of substrate (Kropp and Richardson, 2003). As noted above, for NEST, no preincubation with paraoxon or paraoxon plus mipafox was required (Kropp *et al*., 2004).

Measurement of NEST Aging

This procedure was adapted from Kropp *et al*., (2004) and Jokanovic *et al*., (1998). Aliquots of brain S9 fraction or NEST preparations were diluted using the same conditions as described above for NTE/NEST activity determination. The aliquots were inhibited for 2 min with the test OP compound at concentrations required to yield ≥ 90% inhibition at 37 °C. The enzyme solution was diluted 1:100 (v/v) with Tris-HCl buffer and allowed to age for timed intervals from 0–15 min, because NTE ages rapidly. At each time point, 400 mM KF was added to a final concentration of 200 mM for specified time intervals, and 400 mM KCl was added (1:1) to paired aliquots to a final concentration of 200 mM to serve as a control. Residual NTE/NEST enzyme activity was measured as described above.

Calculation of Bimolecular Rate Constant of Inhibition, k_i

The apparent bimolecular rate constants of inhibition (k_i) of the OP inhibitors against the esterase enzymes were determined as follows (Doorn *et al*., 2003; Kropp and Richardson, 2003; Richardson, 1992). The reaction with inhibitor (I) was carried out so that $[I] > 10$ [enzyme] and $[I] << K_a$, where K_a is the Michaelis-type association constant between the enzyme and inhibitor. These conditions were used to ensure that pseudo-first-order kinetics could be met. The slopes of the primary linear kinetic plots of ln(% activity) vs time were the apparent first-order rate constants of inhibition (k') for each [I]. The slope of the secondary linear kinetic plot of $-k'$ vs [I] is the k_i for the inhibitor. Plots and regressions were carried out using Prism version 3.0–5.0 for Windows, GraphPad Software, Inc. (San Diego, CA), although another suitable statistical/graphics program may be used.

Calculation of First-Order Rate Constant of Aging, k_4

The first-order rate constant of aging (k_4) was determined by the amount of esterase activity that could not be reactivated by 2-PAM versus buffer or KF versus KCl (Jianmongkol *et al*., 1999; Kropp and Richardson, 2006; Kropp *et al*., 2004; Richardson, 1992). The % reactivation was determined by the equation, $[(AR_t) - (AI_t)/(AR_o) - (AI_o)] \times 100$, where AR_t was the activity of reactivated enzyme at t_{aging}, AI_t was the activity of inhibited enzyme without 2-PAM or KF at t_{aging}, AR_o was the activity of the reactivated enzyme at t_o, and AI_o was the activity of inhibited enzyme without 2-PAM or KF at t_o. By using the equation $\ln(100/\%\text{reactivation}) = k_4 \times t_{aging}$, the plot of ln(100/%reactivation) vs t gives a straight line with a slope = k_4.

Results

Tables 3.1 and 3.2 list the k_i data obtained in the present study for CPS, CPO, DFP, and MIP against AChE and NTE or NEST from different species (hen, mouse, and recombinant human). There was good agreement in inhibitory potency for a given inhibitor across species for AChE and for NTE or NEST. Moreover, correlations of k_i values for either mouse brain or human recombinant enzymes with those for hen brain enzymes were excellent (Figures 3.1 and 3.2).

Table 3.3 shows the RIP values calculated from the respective k_i data given in Tables 3.1 and 3.2. All three enzymes show that CPO is highly cholinergic (RIP >> 1), DFP is slightly cholinergic (RIP > 1), and MIP is slightly neuropathic (RIP < 1). There were excellent correlations of RIP values for hen brain enzymes with RIP values from either mouse brain or human recombinant enzymes (Figure 3.3).

Rates of aging were determined only for hrNEST. As expected, MIP was found to be refractory to reactivation by KF; in addition, DFP and CPO were found to have first-order rate constants of aging (k_4) of 0.112 and 0.161 min^{-1} respectively.

Discussion

Using the methods described above, neuropathic potential can be predicted using the S9 fractions from hen or mouse brain homogenates, or preparations of human recombinant AChE and NEST. The inhibitors tested were chlorpyrifos (CPS), chlorpyrifos oxon (CPO), diisopropylphosphorofluoridate (DFP), and mipafox (MIP).

These inhibitors were chosen, because CPS is a pro-toxicant (meaning it must be metabolized to CPO to inhibit the esterases, thus serving as a control) (Richardson, 1995); CPO is a predominantly cholinergic OP, and DFP and MIP are intermediate between cholinergic and neuropathic, each capable of producing OPIDN (Kropp and Richardson, 2003). The ability for an OP to produce OPIDN is based on the relative inhibitory potency (RIP) toward AChE and NTE given by the ratio, k_i(AChE)/k_i(NTE). If the RIP is greater than one, then the compound will cause a lethal cholinergic toxicity, and cannot produce OPIDN at doses less than the LD50; however, if the RIP is less than one, then the compound has the potential to cause OPIDN (Kropp and Richardson, 2003; Lotti and Johnson, 1978; Malygin *et al*., 2003; Richardson, 1992; Richardson *et al*., 1993).

Because previously reported inhibitory potencies have often been fixed-time IC_{50} values, in order to compare our kinetically determined potencies with the literature, we have converted k_i values into IC_{50} values, as shown in Tables 3.1 and 3.2. The range of literature values for hen brain enzymes inhibited by CPO are shown in Table 3.5. The fixed-time inhibition values calculated for the hen brain enzymes in this experiment are consistent with these values by either falling within the range or being within one standard error.

The range of literature values for mouse brain enzymes are shown in Table 3.6. The calculated fixed-time inhibition values are again in good agreement for DFP and MIP. The calculated IC_{50} values are lower in this study for CPO than those previously published; however, it should be noted that the values reported by both Ehrich and Quistad had different conditions. The study performed by Ehrich *et al.,* (1997) used

murine neuroblastoma cells incubated with OP compounds for one hour, and had inherent differences in IC_{50} values. The investigations by Quistad *et al.,* (2001, 2002) calculated the IC_{50} at 25 °C for 15 minutes. The 15 minute IC_{50} value calculated from the k_i value adjusted for temperature, is 9.81×10^{-9} M, more closely aligns to the reported literature value.

The range of literature values for human or human recombinant enzymes are shown in Table 3.7. The calculated values for this study aligned with literature values, except for NTE inhibited by CPO, which was reported in the literature 10X lower than what was calculated. The solitary value found in the literature for human NTE or NEST inhibited by CPO was by Ehrich *et al.,* (1997), and was determined using human neuroblastoma cells.

Overall, the k_i values determined *in vitro* in this study agree well with literature values. When comparing the values to those determined from neuroblastoma tissues, there are some discrepancies. This does not discourage the correspondence since the correlations between the species and with other literature data are still strong. The calculated RIP value of CPO is much larger than 1, meaning that it is not likely to cause OPIDN. The RIP of DFP is slightly larger than 1 and MIP is slightly lower than 1, which signifies that it is more likely to neuropathies. These results also correspond with data that were previously published (Lotti and Johnson, 1978; Kropp and Richardson, 2003). Furthermore, earlier studies of OP compounds *in vitro* have shown similar correlations in inhibitory potential of human and hen brain tissues and neuroblastoma cell lines of both human and mice (Lotti and Johnson, 1978, Ehrich, 1997). By directly comparing human recombinant proteins and chicken and mouse brain tissues, a correlation was established

between all three species, and as a result any of these systems could be used reliably to investigate neuropathic potential.

To further investigate the kinetics of OP compound interactions with AChE and NTE among the three species, it would be important to characterize post inhibitory reactions. In this study, the rate of aging was calculated for hrNEST using all three inhibitors, and agreed with studies that had been published by our laboratory for MIP and DFP (Kropp *et al.,* 2004; Kropp and Richardson, 2006). Literature values for aging of hbNTE inhibited by DFP report $t_{1/2}$ of < 10 min and conclude rapid aging of this enzyme (Clothier and Johnson, 1980, Jokanovic *et al.*, 1998). There appears to be no *in vitro* kinetic data for mbNTE calculating the rate of aging. By determining the rate of aging for mouse brain and hen brain, there can be further correlations made with the kinetic properties of the enzymes between all three species.

In order to model OPIDN, >70% of NTE must be inhibited and aged in hens, and this can be induced in a single dose (Johnson, 1982). The association of inhibitor profile and manifestation of OPIDN closely correlating with known human exposures makes hens the standard for OP compound testing. *In vivo* studies in mice have proved to be more difficult; initially it appeared that OPIDN could be produced only if a neuropathic compound were administered chronically (Lapadula, 1985). A delayed neurotoxicity is also observed clinically in mice 10 hrs after given an acute dose of a neuropathic compound that irreversibly inhibits >80% of NTE (Wu and Casida, 1996). This presentation is not associated with histopathological analysis. Nevertheless, this protein is necessary for the proper neural development and maintenance, because complete deletion of NTE in mice by conventional knockout procedures produces an embryonic lethal

phenotype due to impaired vasculogenesis (Moser *et al.,* 2004) and conditional deletion of NTE within the central nervous system during late embryogenesis leads to neurodegeneration (Akassoglou *et al.,* 2004).

In conclusion, although hens have been historically used as the standard for testing of neuropathic compounds due to the similarities with humans, these data support mice homogenates and human recombinant enzymes may serve as an *in vitro* model of neuropathic potential. An *in vivo* model using mice may be developed, but it would first be important to establish a method to overcome the high threshold necessary to produce the phenotypic delayed neurotoxicity and a metabolic activation system.

Table 3.1. Bimolecular rate constants of inhibition (k_i) and corresponding fixed-time IC_{50} values for organophosphorus inhibitors against acetylcholinesterase (AChE) from different species.[a]

Inhibitor[b]	**Enzyme**[c]					
	hbAChE		mbAChE		hrAChE	
	k_i	IC_{50}	k_i	IC_{50}	k_i	IC_{50}
MIP	$1.07 \pm 0.01 \times 10^{3}$	$3.23 \pm 0.05 \times 10^{-5}$	$4.86 \pm 0.57 \times 10^{2}$	$7.33 \pm 0.86 \times 10^{-5}$	$2.29 \pm 0.06 \times 10^{3}$	$1.52 \pm 0.04 \times 10^{-5}$
DFP	$1.43 \pm 0.05 \times 10^{5}$	$2.43 \pm 0.09 \times 10^{-7}$	$9.89 \pm 0.61 \times 10^{4}$	$3.53 \pm 0.23 \times 10^{-7}$	$1.11 \pm 0.11 \times 10^{5}$	$3.17 \pm 0.30 \times 10^{-7}$
CPO	$1.06 \pm 0.07 \times 10^{7}$	$3.30 \pm 0.22 \times 10^{-9}$	$1.13 \pm 0.03 \times 10^{7}$	$3.06 \pm 0.08 \times 10^{-9}$	$1.30 \pm 0.08 \times 10^{7}$	$2.69 \pm 0.17 \times 10^{-9}$
CPS	NI at 0.10 mM		NI at 0.10 mM		NI at 0.10 mM	

[a] Values are means ± SEM ($M^{-1}min^{-1}$ for k_i, M for IC_{50}). $IC_{50}=ln(2)/k_i \times t$ where t = 20 min. Number of separate experiments (n) shown in parentheses. NI = no inhibition at the highest concentration tested (0.1 mM).
[b] CPS = chlorpyrifos; CPO = chlorpyrifos oxon; DFP = diisopropylphosphorofluoridate; MIP = mipafox.
[c] hbAChE = hen brain AChE; mbAChE = mouse brain AChE; hrAChE = human recombinant AChE.

Table 3.2. Bimolecular rate constants of inhibition (k_i) and corresponding fixed-time IC_{50} values for organophosphorus inhibitors against neuropathy target esterase (NTE) or NTE catalytic domain (NEST) from different species.[a]

Inhibitor[b]	**Enzyme**[c]					
	hbNTE		mbNTE		hrNEST	
	k_i	IC_{50}	k_i	IC_{50}	k_i	IC_{50}
MIP	$4.02 \pm 0.24 \times 10^{3}$	$8.69 \pm 0.54 \times 10^{-6}$	$1.08 \pm 0.09 \times 10^{3}$	$3.26 \pm 0.27 \times 10^{-5}$	$4.34 \pm 0.14 \times 10^{3}$	$8.01 \pm 0.25 \times 10^{-6}$
DFP	$6.37 \pm 0.26 \times 10^{4}$	$5.46 \pm 0.23 \times 10^{-7}$	$3.08 \pm 0.39 \times 10^{4}$	$1.16 \pm 0.14 \times 10^{-6}$	$3.75 \pm 0.24 \times 10^{4}$	$9.35 \pm 0.66 \times 10^{-7}$
CPO	$4.00 \pm 0.76 \times 10^{5}$	$9.57 \pm 1.65 \times 10^{-8}$	$4.53 \pm 1.09 \times 10^{5}$	$8.43 \pm 1.65 \times 10^{-8}$	$1.54 \pm 0.33 \times 10^{5}$	$2.25 \pm 0.41 \times 10^{-7}$
CPS	NI at 0.10 mM		NI at 0.10 mM		NI at 0.10 mM	

[a] Values are means ± SEM ($M^{-1}min^{-1}$ for k_i, M for IC_{50}). IC_{50} values calculated using the equation $IC_{50}=ln(2)/k_i \times t$ where t = 20 minutes. Number of separate experiments (n) shown in parentheses. NI = no inhibition at the highest concentration tested (0.1 mM).

[b] CPS = chlorpyrifos; CPO = chlorpyrifos oxon; DFP = diisopropylphosphorofluoridate; MIP = mipafox.

[c] hbNTE = hen brain NTE; mbNTE = mouse brain NTE; hrNEST = human recombinant NEST.

Table 3.3. Relative inhibitory potential (RIP) for organophosphorus inhibitors against acetylcholinesterase (AChE) versus neuropathy target esterase (NTE) or NTE catalytic domain (NEST) from different species.[a]

Inhibitor[b]	**Enzyme**		
	Hen Brain (hb)	Mouse Brain (mb)	Human Recombinant (hr)
MIP	0.267 ± 0.016	0.452 ± 0.064	0.526 ± 0.022
DFP	2.24 ± 0.121	3.21 ± 0.449	2.96 ± 0.352
CPO	26.5 ± 5.36	25.0 ± 6.06	84.3 ± 19.1

[a] Data are mean ± SEM. RIP = [k_i(AChE)/k_i(NTE or NEST)], where k_i = bimolecular rate constants of inhibition; n = 3 – 4 for each k_i (from Tables 1 and 2).
[b] CPO = chlorpyrifos oxon; DFP = diisopropylphosphorofluoridate; MIP = mipafox.

Table 3.4. Rate constant of aging (k_4) and calculated half-time ($t_{1/2}$) for neuropathy target esterase catalytic domain (NEST)[a]

Inhibitor[b]	k_4	$t_{1/2}$
MIP	no reactivation	*n.d.*
DFP	0.112 ± 0.037	6.18
CPO	0.161 ± 0.044	4.30

n.d. Value not determined. There was no reactivation at any time point as MIP-NEST appears to age instantaneously

[a] Data are mean ± SEM (min^{-1} for k_4, min for $t_{1/2}$). $t_{1/2} = ln(2)/k_4$. $n = 3$.

[b] CPO = chlorpyrifos oxon; DFP = diisopropylphosphorofluoridate; MIP = mipafox.

Table 3.5. Reported or calculated fixed-time IC_{50} values (M) for hen brain neuropathy target esterase (NTE) and acetylcholinesterase (AChE)[a]

Inhibitor[b]	Reported IC_{50} values NTE	AChE	References
MIP	9.6 - 6.1 x 10^{-6}	41.2 - 8.6 x 10^{-6}	Richardson *et al.,* 1993[c] Kropp *et al.,* 2003[d]
DFP	7 - 5.6 x 10^{-7}	6.2 x 10^{-7}	Lotti and Johnson, 1978[e] Atkins and Glynn, 2000[f]
CPO	3.49 - 1.45 x 10^{-7}	2.30 - 1.95 x 10^{-9}	Lotti and Johnson, 1978 Correll *et al.,* 1987[g] Atkins and Glynn, 2000 Kropp and Richardson, 2003[h]

[a] IC_{50} values derived from the literature or calculated from reported bimolecular rates of inhibition (k_i) using the equation $IC_{50}=\ln(2)/k_i \times t$ where time (t) is 20 min.
[b] MIP = mipafox; DFP = diisopropylphosphorofluoridate; CPO = chlorpyrifos oxon.
[c] Richardson *et al.* reported k_i values.
[d] Kropp *et al.* reported k_i values.
[e] Lotti and Johnson reported 20 minute IC_{50} values.
[f] Atkins and Glynn reported 20 minute IC_{50} values.
[g] Correll *et al.* reported IC_{50} values of undetermined time.
[h] Kropp and Richardson reported k_i values.

Table 3.6. Reported or calculated fixed-time IC_{50} values (M) for mouse brain neuropathy target esterase (NTE) and acetylcholinesterase (AChE)[a]

	Reported IC_{50} values		
Inhibitor[b]	**NTE**	**AChE**	**References**
MIP	$120 – 5.7 \times 10^{-6}$	4.6×10^{-5}	Ehrich *et al.,* 1997[c] Quistad *et al.,* 2001[d]
DFP	$12 - 3.0 \times 10^{-7}$	$900 – 5.6 \times 10^{-8}$	Ehrich *et al.,* 1997 Quistad *et al.,* 2002[d]
CPO	9.6×10^{-7}	$1.9 – 1.1 \times 10^{-8}$	Ehrich *et al.,* 1997 Quistad *et al.,* 2002

[a] IC_{50} values derived from the literature or calculated from reported bimolecular rates of inhibition (k_i) using the equation $IC_{50}=\ln(2)/k_i \times t$ where time (t) is 20 min.
[b] MIP = mipafox; DFP = diisopropylphosphorofluoridate; CPO = chlorpyrifos oxon.
[c] Ehrich *et al.,* reported 60 minute IC_{50} values derived from murine neuroblastoma cell line enzymes.
[d] Quistad *et al.,* reported 15 minute IC_{50} values derived from mouse brain homogenate enzymes.

Table 3.7. Reported or calculated fixed-time IC_{50} values (M) for human brain neuropathy target esterase (NTE) or NTE catalytic domain (NEST) and acetylcholinesterase (AChE)[a]

	Reported IC_{50} values		
Inhibitor[b]	**NTE / NEST**	**AChE**	**References**
MIP	$18.4 – 8.7 \times 10^{-6}$	$13 – 2.36 \times 10^{-6}$	Ehrich *et al.,* 1997[c] Amitai *et al.,* 1998[d]
DFP	$20.1 – 9.6 \times 10^{-7}$	$83 – 2.0 \times 10^{-8}$	Lotti and Johnson, 1978[e] Ehrich *et al.,* 1997 Atkins and Glynn, 2000[f] Kropp *et al.,* 2004[g] Kropp and Richardson, 2006[h]
CPO	6.9×10^{-8}	$37.3 - 3.4 \times 10^{-10}$	Lotti and Johnson, 1978 Ehrich *et al.,* 1997 Atkins and Glynn, 2000 Kropp *et al.,* 2004 Kropp and Richardson, 2006

[a] IC_{50} values derived from the literature or calculated from reported bimolecular rates of inhibition (k_i) using the equation $IC_{50}=\ln(2)/k_i \times t$ where time (t) is 20 min.
[b] MIP = mipafox; DFP = diisopropylphosphorofluoridate; CPO = chlorpyrifos oxon.
[c] Ehrich *et al.* reported 60 minute IC_{50} values derived from human neuroblastoma cell NTE and AChE.
[d] Amitai *et al.* reported k_i values derived from human recombinant AChE.
[e] Lotti and Johnson reported 20 minute IC_{50} values derived from human brain homogenate NTE and AChE.
[f] Atkins and Glynn reported 20 minute IC_{50} values derived from human recombinant NEST.
[g] Kropp *et al.* reported k_i values derived from NEST.
[h] Kropp and Richardson reported k_i values derived from NEST.

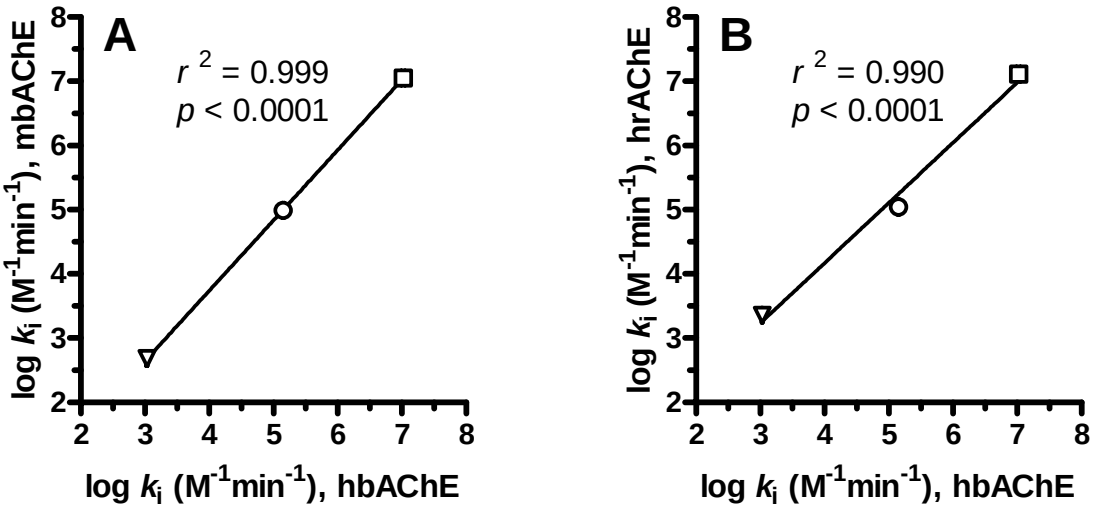

Figure 3.1. Correlation of log k_i hbAChE with (A) log k_i mbAChE and (B) hrAChE, where k_i = bimolecular rate constant of inhibition ($M^{-1}min^{-1}$). AChE = acetylcholinesterase; hb = hen brain; mb = mouse brain; hr = human recombinant. Symbols: triangles = mipafox (MIP); circles = diisopropylphosphorofluoridate (DFP); squares = chlorpyrifos oxon (CPO). Each data point corresponds to a mean value ± SEM in both the x and y directions.

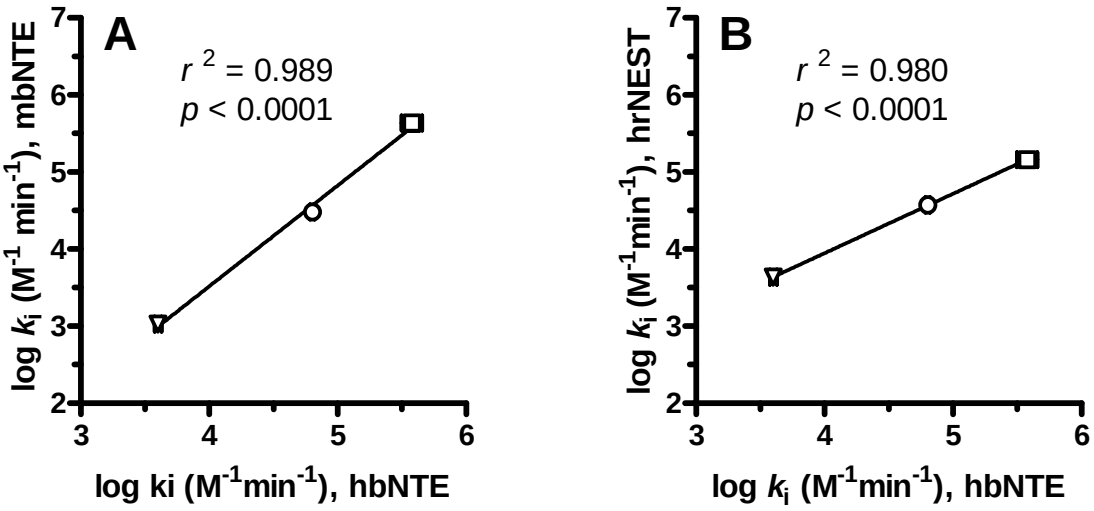

Figure 3.2. Correlation of log k_i hbNTE with (A) log k_i mbNTE and (B) hrNEST, where k_i = bimolecular rate constant of inhibition ($M^{-1}min^{-1}$). NTE = neuropathy target esterase; NEST = NTE catalytic domain; hb = hen brain; mb = mouse brain; hr = human recombinant. Symbols: triangles = mipafox (MIP); circles = diisopropylphosphorofluoridate (DFP); squares = chlorpyrifos oxon (CPO). Each data point corresponds to a mean value ± SEM in both the x and y directions.

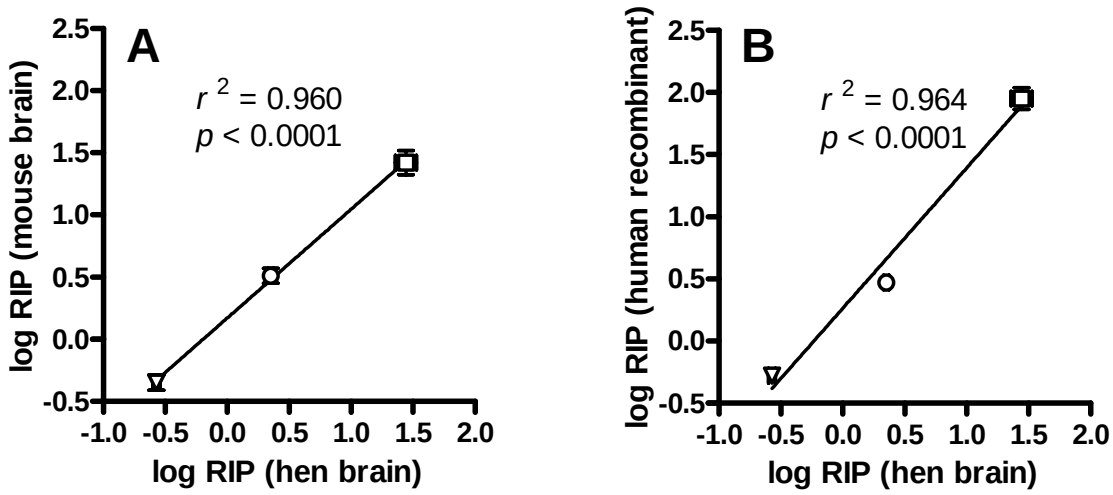

Figure 3.3. Correlation of log RIP (hen brain) with (A) log RIP (mouse brain) and (B) log RIP (human recombinant), where RIP = [k_i(AChE)/k_i(NTE or NEST)]; k_i = bimolecular rate constants of inhibition ($M^{-1}min^{-1}$); n = 3 – 4 for each k_i (from Tables 1 and 2). AChE = acetylcholinesterase; NTE = neuropathy target esterase; NEST = NTE catalytic domain. Symbols: triangles = mipafox (MIP); circles = diisopropylphosphorofluoridate (DFP); squares = chlorpyrifos oxon (CPO). Each data point corresponds to a mean value ± SEM in both the x and y directions.

References

Abou-Donia, M.B. (1981). Organophosphorus ester-induced delayed neurotoxicity. *Annu. Rev. Pharmacol. Toxicol.* **21,** 511-548.

Akassoglou, K., Malester, B., Xu, J., Tessarollo, L., Rosenbluth, J., and Chao, M.V. (2004). Brain-specific deletion of neuropathy target esterase/swisscheese results in neurodegeneration. *PNAS* **101,** 5075-5080.

Amitai, G., Moorad, D., Adani, R., and Doctor, B.P. (1998). Inhibition of acetylcholinesterase and butyrylcholinesterase by chlorpyrifos-oxon. *Biochem. Pharmacol.* **56,** 293-299.

Atkins, J., and Glynn, P. (2000). Membrane association of and critical residues in the catalytic domain of human neuropathy target esterase. *J. Biol. Chem*. **275**, 24477-24483.

Atkins, J., Luthjens, L. H., Hom, M. L., and Glynn, P. (2002). Monomers of the catalytic domain of human neuropathy target esterase are active in the presence of phospholipid. *Biochem. J.* **361**, 119-123.

Clothier, B. and Johnson, M.K. (1980). Reactivation and aging of neurotoxic esterase inhibited by a variety of organophosphorus esters. *Biochem. J.* **185,** 739-747.

Correll, L., and Ehrich, M. (1987). Comparative sensitivities of avian neural esterases to in vitro inhibition by organophosphorus compounds. *Toxicol. Lett.* **36,** 197-204.

Doorn, J.A., Thompson, C.M., Christner, R.B., and Richardson, R.J. (2003). Stereoselective interaction of *Torpedo californica* acetylcholinesterase by isomalathion: Inhibitory reactions with (1*R*)- and (1*S*)-isomers proceed by different mechanisms. *Chem. Res. Toxicol.* **16**, 958-965.

Ehrich, M., Correll, L., Veronesi, B. (1997). Acetylcholinesterase and neuropathy target esterase inhibitions in neuroblastoma cells to distinguish organophosphorus compounds causing acute and delayed neurotoxicity. *Fund. Appl. Toxicol.* **38,** 55-63.

Ellman, G., Courtney, K. D., Andres, V. Jr., and Featherstone, R. M. (1961). A new and rapid colorimetric determination of acetylcholinesterase activity. *Biochem. Pharmacol*. **7**, 88–95.

Jianmongkol, S., Berkman, C.E., Thompson, C.M., and Richardson, R.J. (1996). Relative potencies of the four stereoisomers of isomalathion for inhibition of hen brain acetylcholinesterase and neurotoxic esterase in vitro. *Toxicol. Appl. Pharmacol*. **139**, 342-348.

Jianmongkol, S., Marable, B.R., Berkman, C.E., Talley, T.T., Thompson, C.M., and Richardson, R.J. (1999). Kinetic evidence for different mechanisms of acetylcholinesterase inhibition by (1*R*)- and (1*S*)-stereoisomers of isomalathion. *Toxicol. Appl. Pharmacol*. **155**, 43-53.

Johnson, M.K. (1982). The target for initiation of delayed neurotoxicity by organophosphorus esters: biochemical studies and toxicological applications. *Rev. Biochem. Toxicol.* **4,** 141-212.

Jokanovic, M., Stepanovic, R.M., Maksimovic, M., Kosanovic, M., and Stojiljkovic, M.P. (1998). Modification of the rate of aging of diisopropylfluorophosphate-inhibited neuropathy target esterase of hen brain. *Toxicol. Lett.* **95**, 93-101.

Kayyali, U.S., Moore, T.B., Randall, J.C., and Richardson, R.J. (1991). Neurotoxic esterase (NTE) assay: optimized conditions based on detergent-induced shifts in the phenol/4-aminoantipyrine chromophore spectrum. *J. Anal. Toxicol.* **15**, 86-89.

Kropp, T.J., and Richardson, R.J. (2003). Relative inhibitory potencies of chlorpyrifos oxon, chlorpyrifos methyl oxon, and mipafox for acetylcholinesterase versus neuropathy target esterase. *J. Toxicol. Environ. Health A* **66**, 1145-1157.

Kropp, T. J., Glynn, P., and Richardson, R. J. (2004). The mipafox-inhibited catalytic domain of human neuropathy target esterase ages by reversible proton loss. *Biochemistry* **43**, 3716-3722.

Kropp, T.J., and Richardson, R.J. (2006). Aging of mipafox-inhibited human acetylcholinesterase proceeds by displacement of both isopropylamine groups to yield a phosphate adduct. *Chem. Res. Toxicol*. **19**, 334-339.

Lapadula, D.M., Patton, S.E., Campbell, G.A., and Abou-Donia, M.B. (1985). Characterization of delayed neurotoxicity in the mouse following chronic oral administration of tri-*o*-cresyl phosphate. *Toxicol. Appl. Pharmacol.* **79,** 83-90.

Lotti, M., and Johnson, M.K. (1978). Neurotoxicity of organophosphorus pesticides: Predictions can be based on *in vitro* studies with hen and human enzymes. *Arch. Toxicol*. **41,** 215-221.

Malygin, V.V., Sokolov, V.B., Richardson, R.J., and Makhaeva, G.F. (2003). Quantitative structure-activity relationships predict the delayed neurotoxicity potential of a series of *O*-alkyl-*O*-methylchloroformimino phenylphosphonates. *J. Toxicol. Environ. Health Part A* **66**, 611-625.

Moser, M., Yong, L., Vaupel, K., Kretzschmar, D., Kluge, R., Glynn, P., and Buettner, R. (2004). Placental failure and impaired vasculogenesis result in embryonic lethality for neuropathy target esterase-deficient mice. *Molec. Cell Biol.* **24,** 1667-1679.

Moretto, A., and Lotti, M. (2002). The relationship between isofenphos cholinergic toxicity and the development of polyneuropathy in hens and humans. *Arch. Toxicol.* **76,** 367-375.

Pomeroy-Black M.J., Jortner, B.S., and Ehrich, M.F. (2007). Early effects of neuropathy-inducing organophosphates on in vivo concentrations of three neurotrophins. *Neurotox. Res.* **11,** 85-91.

Quistad, G.B., Sparks, S.E., and Casida, J.E. (2001). Fatty acid amide hydrolase inhibition by neurotoxic organophosphorus pesticides. *Toxicol. Appl. Pharmacol.* **173,** 48-55.

Quistad, G.B., Sparks, S.E., Segall, Y., Nomura, D.K., and Casida, J.E. (2002). Selective inhibitors of fatty acid amide hydrolase relative to neuropathy target esterase and acetylcholinesterase: Toxicological implications. *Toxicol. Appl. Pharmacol*. **179**, 57-63.

Richardson, R.J. (1995). Assessment of the neurotoxic potential of chlorpyrifos: A critical review of the literature. *J. Toxicol. Environ. Health* **44**, 135-165.

Richardson, R. J. (2005). Organophosphate Poisoning, Delayed Neurotoxicity. In *Encyclopedia of Toxicology, 2nd Edition* (4 vols.) (P. Wexler, ed.), Vol. 3, pp. 302-306, Elsevier, Ltd., Oxford.

Richardson, R.J., Moore, T.B., Kayyali, U.S., Fowke, J.H., and Randall, J.C. (1993). Inhibition of hen brain acetylcholinesterase and neurotoxic esterase by chlorpyrifos *in vivo* and kinetics of inhibition by chlorpyrifos oxon *in vitro*: application to assessment of neuropathic risk. *Fundam. Appl. Toxicol*. **20**, 273-279.

USEPA (1998). Health Effects Test Guidelines. OPPTS 870.6100. Acute and 28-day delayed neurotoxicity of organophosphorus substances. EPA 712-C-98-237, U.S. Government Printing Office, Washington, DC; USEPA (http://www.epa.gov/epahome/research.htm).

van Tienhoven, M., Atkins, J., Li, Y., and Glynn, P. (2002). Human neuropathy target esterase catalyzes hydrolysis of membrane lipids. *J. Biol. Chem.* **277**, 20942-20948.

Veronesi, B., Padilla, S., Blackmon, K., and Pope, C. (1991). A murine model of OPIDN: Neuropathic and biochemical description. *Toxicol. Appl. Pharmacol.* **107,** 311-324.

Wu, S.-Y., and Casida, J.E. (1996). Subacute neurotoxicity induced in mice by potent organophosphorus neuropathy target esterase inhibitors. *Toxicol. Appl. Pharmacol.* **139,** 195-202.

CHAPTER 4

HUMAN RECOMBINANT NEUROPATHY TARGET ESTERASE DOMAIN CONTAINING MUTATIONS RELATED TO MOTOR NEURON DISEASE HAVE ALTERED ENZYMATIC PROPERTIES

Abstract

Neuropathy target esterase (NTE) is a lysophospholipase hydrolase protein, which is associated with organophosphorus (OP) compound delayed neurotoxicity (OPIDN). Distal axonopathies of sensory and motor neurons are physiological manifestations of some types of paraplegia and OPIDN. An investigation of this similarity in disease presentation led to a recent discovery of mutations within the esterase domain of NTE in patients who were affected with a particular hereditary spastic paraplegia, named NTE-related motor neuron disease (NTE-MND). Two of these mutations, R890H and M1012V, were created in human recombinant neuropathy target esterase domain (NEST) to measure possible changes in catalytic properties. These mutated enzymes had decreased specific activities for hydrolysis of the artificial substrate, phenyl valerate. In addition, the bimolecular rate constants of inhibition were reduced. Finally, mutated enzymes inhibited by OP compounds exhibited altered kinetics of aging (time-dependent loss of the ability to be reactivated by nucleophiles). These data suggest that the

mutations created in association with NTE-MND have a functional correlate in altered enzymological properties of NTE.

Introduction

Neuropathy target esterase (NTE) was first recognized as a serine hydrolase that covalently binds certain organophosphorus (OP) compounds that produce a delayed axonopathy in adult vertebrates (Johnson, 1969). Clinical manifestations OP compound-induced delayed neurotoxicity (OPIDN) become apparent 1-4 weeks after exposure to a neuropathic OP compound, and are consistent with a Wallerian-type distal axonopathy, a wave-like and active process of degeneration that progresses in a proximal-to-distal direction (Davis and Richardson, 1980; Beirowski *et al*., 2005). Symptoms of OPIDN include paresthesias in the distal extremities, sensory loss, ataxia, and flaccid paralysis, and eventual reinnervation of the muscle with persistent lesions in descending upper motor neuron axons can lead to spastic paralysis (Richardson, 2005; Lotti and Moretto, 2005). OPIDN is associated with the inhibition of >70% of NTE by neuropathic compounds and aging of the NTE-OP conjugate. The processes of inhibition and aging are illustrated in Figure 4.1 (Glynn, 2006) and the kinetics of these steps can be measured using phenyl valerate as a synthetic substrate (Johnson, 1969). Although the precise mechanism of toxicity is unknown, NTE belongs to a group of lysophophospholipases, which are thought to maintain membrane integrity. Thus, disruption of NTE activity by OP inhibition and aging could produce a perturbation in the metabolism of membrane

lysophospholipids, potentially leading to axonopathy (Quistad *et al.*, 2003; Vose *et al.,* 2008).

A recent neurogenetic evaluation discovered a familial disease, with physiological presentations of distal motor axonopathies associated with progressive weakness and muscular atrophy, to have three different types of genetic autosomal-recessive mutations in the locus encoding NTE, named NTE-related motor neuron disease (NTE-MND) (Rainier *et al.*, 2008). Two of these defects involved point mutations within the NTE esterase domain (NEST), arginine 890 to histidine (R890H) and methionine 1012 to valine (M1012V), and a third mutation, which was an insertion into a codon that caused a premature stop, and therefore a truncation. Although the focus of human neurodegeneration, NEST is a highly conserved region within NTE found in bacteria, yeast, nematode, *Drosophila*, and mice which further suggests mutations within the region could have neurological implications (Lush *et al.,* 1998).

In order to study the effects of critical residues within NEST, the protein has been expressed in *E. coli*, and purified. Site directed mutagenesis studies of NEST have confirmed serine 966 as the active site serine and shown that two aspartate residues (aspartate 1086 and aspartate 960) are essential for enzymatic activity (Atkins and Glynn, 2000). A homology model of the NTE catalytic domain indicates that serine 966 and aspartate 1086 form the catalytic dyad and that aspartate 960 is predicted to lie on the surface of the molecule (Wijeyesakere et al., 2007). The present study was carried out to test the hypothesis that mutations in the sequence of NEST found in association with NTE-MND will have functional consequences detectable as changes in the kinetics of substrate hydrolysis, inhibition, and aging.

Materials and Methods

Chemicals

N,*N*′-diisopropylphosphorodiamidofluoridate (mipafox, MIP) was synthesized by ChemSyn, and purchased from the Midwest Research Institute (Kansas City, MO). Diisopropylfluorophosphate (DFP) was purchased from Sigma Aldridge (St. Louis, MO). O,O-diethyl O-3,4,5-trichloro-2-pyridyl phosphate (chlorpyrifos oxon, CPO) was furnished by Dow AgroSciences (Indianapolis, IN). Dioleoylphosphatidylcholine (DOPC) was purchased from Avanti (Alabaster, AL).

Protein Expression and Purification

NEST protein and the mutations were expressed and purified using the protocol from Atkins and Glynn with some modification (2000). Cultures were grown in TB media at 37 °C until OD_{600} = 1.0, when the temperature was reduced to 20 °C and the cells were induced with 0.4 mM isopropyl-β-D-thiogalactopyranoside for 16 hr (overnight). The cells were centrifuged for 12 min at 12,000 × *g* at 4 °C and the pellets were stored at −80 °C.

Thawed cell pellets were resuspended in PEN buffer (50 mM sodium phosphate buffer pH 8.0, 300 mM NaCl, and 0.1 mM EDTA) containing 3% (w/v) 3-[(3-cholamidopropyl)dimethylammonio]-1-propanesulfonate (CHAPS), and sonicated at 30 sec intervals for 5 min with an output of 25 mA. The resulting mixture was centrifuged at 20,000 × *g* for 60 min at 4 °C. The supernatant was absorbed onto nickel-nitrilotriacetic

acid-agarose and washed three times with PEN buffer containing 0.3% (w/v) CHAPS and three times with PEN buffer containing 0.3% (w/v) CHAPS and 10 mM imidazole. The protein was eluted with PEN buffer containing 0.3% (w/v) CHAPS and 300 mM imidazole. The protein was then diluted to 0.1 mg/mL and dialyzed 3 × 100 in PEN buffer containing 1mM dithiothreitol at 4 °C, the first two for 2 hr, the last one overnight. The purification was monitored on SDS-PAGE, and protein concentration was determined using A280 on NanoDrop ND-1000 UV/Vis spectrophotometer (Thermo Scientific, Wilmington, DE)

Site-Directed Mutagenesis:

Site-directed mutagenesis was performed using the QuikChange II Site-Directed Mutagenesis kit from Stratagene (La Jolla, CA) to create the HSP mutations arginine 890 to histidine (R890H) and methionine 1012 to valine (M1012V) with primers purchased from Invitrogen. The forward primer used for the R890H mutation was 5′-GCACCTGCGCTGTCCGCACCGCCTCTTTTCGCGC-3′; the reverse primer was 5′-GCGCGAAAAGAGGCGGTGCGGACAGCGCAGGTGC-3′. The forward primer for the M1012V mutation was 5′-CGTACCCAGTCACCTCCGTGTTCACTGGGTCTGCC-3′; reverse primer was 5′-GGCAGACCCAGTGAACACGGAGGTGACTGGGTACG-3′. A polymerase chain reaction was set up using *Pfu* DNA polymerase (Stratagene). The plasmid was then subcloned into the pET21b vector, expressed in competent DH5α *E. coli* cells, and isolated using QIAprep from QIAGEN. The mutations were verified by DNA sequencing at the University of Michigan Core Facility (Ann Arbor, MI).

Determination of NEST activity

The activity of NEST was determined by a colorimetric assay as described by Johnson (1977) and Kayyali *et al.* (1991), without the use of inhibitors. All reactions were carried out at 37 °C for the entire assay. Aliquots of NEST were diluted in buffer containing 50 mM Tris-HCl and 0.1 mM EDTA, pH = 8.0 at 25°C. The substrate solution of 5.3 mM phenyl valerate / *N*,*N*′-dimethylformamide (PV/DMF) diluted in 0.03% Triton X-100 (w/v) was added, and the reaction was allowed to proceed for 20 min. A stop solution of 9.5 mg/mL sodium dodecyl sulfate /11.23 mM 4-aminoantipurine was added and the reaction with the phenol produced was allowed to proceed for 5 min. A solution of 12.1 mM $K_3Fe(CN)_6$ was added and color was allowed to develop and stabilize for 10 min. The endpoint absorbance was measured at 486 nm using a SpectraMax 340 microplate reader (Molecular Devices, Sunnydale, CA).

Calculation of k_i

The apparent bimolecular rate constants of inhibition (k_i) of the OP inhibitors against the NEST enzymes were determined as previously described (Aldridge and Reiner, 1972; Richardson and Kropp, 2003). The reaction with inhibitor (*I*) was carried out so that [*I*] > 10 [enzyme] and [*I*] << K_d. These conditions were used so that k_i can be measured using linear regression to model pseudo-first-order kinetics. The slopes of the primary linear kinetic plots of ln(%activity) vs time were the apparent first-order rate constants of inhibition (*k'*) for each [*I*]. The slope of the secondary linear kinetic plot of –*k'* vs [*I*] was the k_i for the inhibitor. Plots and regressions were carried out using Prism version 5.0 for Windows, GraphPad Software, Inc. (San Diego, CA).

Determination of NEST aging

Aliquots of NEST were diluted using the same conditions as described for the activity determination, and all assays were performed at 37 °C. The aliquots were inhibited for 2 min with OP compounds at concentrations required to yield 90% inhibition. The enzyme solution was diluted 1:100 (v/v) with Tris-HCl buffer, pH 8.0 at 25 °C to stop inhibition and the reaction was allowed to age for timed intervals from 0-15 minutes. At each time point, KF was added to a final concentration of 200 mM and enzyme was allowed to reactivate for 20 min KCl was added as inhibited nonreactivated control. An uninhibited KCl treated NEST control was also measured. Enzyme activity was measured as described above.

Calculation of k_4

The first-order rate constant of aging (k_4) was described as a ratio of specific activities for inhibited and KF reactivated NEST. The % reactivation was determined by the equation $[(AR_t)-(AI_t)]/[(AR_o)-(AI_o)] \times 100$, where AR_t is the activity of reactivated enzyme at t_{aging}, AI_t is the activity of inhibited enzyme without oxime or KF at t_{aging}, AR_o is the activity of the reactivated enzyme at t_0, and AI_o is the activity of inhibited enzyme without oxime or KF at t_0. The value of k_4 was then determined by the slope of the linear plot of ln(100/% reactivation) against time.

Statistical Analysis

The data are presented as mean ± SEM. The specific activity for each protein was calculated by three paired determinations of protein concentration and phenol produced. The means for specific activity and k_i were compared sing one-way analysis of variance (ANOVA) and Tukey post hoc test for multiple comparisons ($p<0.05$). Data and comparisons were performed using GraphPad Prism version 5.01 (GraphPad Software, Inc., San Diego, CA)

Results

The PV hydrolase activity of the *wt*NEST was found to be 2.43 mmol phenol produced/mg protein/min, and is similar to what has been reported previously (van Tienhoven *et al.*, 2002). Both of the HSP mutations had significantly reduced PV hydrolase activity compared to the *wt*NEST (Table 4.1), however not to each other. These mutations were not severe enough to abolish all activity.

To investigate additional changes in enzymological properties, the kinetic values of inhibition for MIP, DFP, and CPO (Figure 4.2) were determined (Table 4.2). These chemicals were chosen because they represented a range of inhibitory potencies and structure, which had been previously established in the literature (Table 4.3). R890H and M1012V both had statistically reduced k_i values for MIP and DFP. Interestingly, the k_i value for CPO was reduced approximately 10-fold in the M1012V mutation, but statistically unchanged in the R890H mutation. All k_i values for M1012V were lower than both the control and the R890H mutation.

The changes in kinetics of inhibition led us to investigate possible changes in post-inhibitory kinetics, specifically the kinetics of aging. The *wt*NEST aged rapidly, with the activity of MIP-inhibited enzyme unable to reactivate at pH 8.0, and the $t_{1/2}$ for aging was 6.18 and 4.30 min for DFP and CPO, respectively. The *wt*NEST activity for the KCl control was approximately 10% of the noninhibited activity, which would be expected since this control was inhibited to the I_{90} and activity would not be restored (Figure 4.3). Analysis of the data for the two mutations did not conform to calculate a kinetic value of aging. The KCl treated controls had a recovery of approximately 20-30% of the specific activity for R890H and 30-60% for M1012V. Furthermore, the inhibited KCl unreactivated control had more hydrolase activity than the KF reactivated species for several of the time points. The MIP inhibited mutants were more reactivated by KCl than by KF, the assumed nucleophilic reactivator. M1012V had more activity in the KCl reactivated wells for all inhibitors at all time points than the KF. R890H had higher activity in the KCl than in the KF after approximately six minutes for both DFP and CPO. The calculation for an appropriate k_4 requires the difference between the reactivated and non-reactivated enzymes to be positive.

Discussion

Mutations of the arginine 890 and methionine 1012 residues within NEST were discovered in patients with NTE-MND (Rainier et al, 2008). Although not previously the focus of homology studies of NTE, arginine 890 is conserved within NTE in humans and the MSWS domain in mice; however, the SWS domain of *Drosophila* and YOL4 of *C.*

elegans contain a K at this residue. The methionine 1012 residue is conserved across mouse, *Drosophila,* and *C. elegans*. The data from the present study show that there is a significant reduction of the PV hydrolase activity in both of the NTE-MND mutations in the NEST domain.. A previously reported site-directed mutagenesis study showed that mutations to serine 966 and aspartates 960 and 1086 abolished hydrolase activity, indicating that these residues are critical for catalysis (Atkins and Glynn, 2000). NTE is essential for embryogenesis and maintenance of proper neuronal function as shown in genetic deletions of the mouse protein (Moser *et al.,* 2004; Akassoglou, 2004). In addition, modest depressions in NTE activity have been associated with a hyperactive phenotype in mice when created by heterozygous ($Nte^{+/-}$) and when chronic dosing with subacute levels of a neuropathic compound (Winrow *et al*., 2003).

Along with reduced specific activity, the NTE-MND also had impairments in kinetic values of inhibition. MIP, DFP, and CPO were chosen because the k_i values reported for NEST and NTE in the literature are spread over a 100 fold range, and they are structurally different from one another. Relative to *wt*NEST, the kinetic values of inhibition for R890H were significantly reduced for MIP and DFP only. The inhibitory values for M1012V were significantly reduced for all three inhibitors compared to both *wt*NEST and R890H. Interestingly, the M1012V mutation had a 10-fold reduction in the kinetic value for CPO. When comparing these values of inhibition to those reported in the literature, the calculated fixed-time IC_{50} values for *wt*NEST concur with the median of the range found published (Table 4.4). The IC_{50} values for R890H are within the reported range for CPO, slightly high for MIP, and on the upper end of the range for DFP. The IC_{50} values for M1012V treated with all three OP compounds are higher than any of

those reported for either hen or human tissues. This change in inhibitory properties reveals further that the NTE-MND mutations have altered the enzymatic function of NEST.

To explore further the deviations in catalytic properties of the mutants from the *wt*NEST, the rates of aging were investigated. The calculated $t_{1/2}$ of aging for *wt*NEST treated with DFP of 6.21 min agrees with previously reported literature values for both NTE and NEST between 3.25 and 7.4 minutes (Clothier *et al*., 1979, Jokanovic *et al.,* 1998, Kropp *et al*., 2004). The rapid and complete aging of mipafox at pH = 8.0 was also previously reported (Kropp *et al.,* 2004). The rate of aging, k_4, could be calculated for *wt*NEST; however, this coefficient could not be appropriately calculated for the mutants. This was because the KCl control, which was to serve as the nonreactivated enzyme, was apparently being reactivated, at times to a greater extent than the KF reactivated enzyme. The most notable deviation is with MIP, where *wt*NEST was clearly nonreactivatable; the mutants were not only reactivated by KF, but the reactivation was higher by KCl. This unexpected behavior of the mutant enzymes could be due to a weakening of the OP-esterase bond being hydrolyzed under simple aqueous dilution, and the released hydrolyzed OP reforming MIP with the excess fluoride ion in solution. We also investigated the possibility that 90% inhibition was not being reached at 2 min with the inhibitor concentrations used; however, a 2-min inhibition curve was performed to confirm that 90% inhibition was indeed being reached (data not shown). Therefore, it seems that the covalent bond between the serine and OP is weakened and more vulnerable to hydrolysis. Further investigations into the rate of reactivation of the NTE-MND mutants with particular inhibitors may agree with this hypothesis.

NTE, along with other and other LPC-hydrolases, maintain a tight homeostasis of phospholipids necessary for cellular membrane integrity. These mutations that were investigated in the present study within the NEST domain affect the kinetics of exogenous substrate activity as well as inhibitory and postinhibitory kinetics. Although this type of inhibitor profiling has not previously been performed on NEST mutants, it has been performed on acetylcholinesterase, where mutations made within the acyl pocket surrounding the active-site gorge altered the inhibitor specificity (Kovarik *et al.*, 2003). In future work, it would be interesting to see if the mutations studied in the present investigation have a similar effect on LPC hydrolysis by NEST or full-length NTE, thus providing further correlation of changes in NTE function with the mutations discovered in NTE-MSD.

Table 4.1. Phenyl valerate (PV) hydrolase activity for neuropathy target esterase (NTE) catalytic domain (NEST) and the NTE-related motor neuron disease mutations, R890H and M1012V[a]

	PV activity[b]	% *wt* NEST
***wt*NEST**	2.43 ± 0.08	100 ± 0.04
R890H	1.74 ± 0.02	71.6 ± 1.01
M1012V	1.55 ± 0.04	64.0 ± 2.02

[a] Data displayed are mean ± SEM, $n = 3$ where PV activity is expressed as mmol phenol produced/mg protein/min

[b] R890H and M1012V were significantly lower than *wt*NEST, but not significantly different from each other.

Table 4.2. Bimolecular rates of inhibition (k_i, $M^{-1}min^{-1}$) and calculated 20 min IC_{50} (μM) values for neuropathy target esterase (NTE) catalytic domain (NEST) and the two NTE-related motor neuron disease mutations, R890H and M1012V[a]

Inhibitor[b]	*wt*NEST		R890H[c]		M1012V[d]	
	k_i	IC_{50}	k_i	IC_{50}	k_i	IC_{50}
MIP	$4.36 \pm 0.13 \times 10^3$	7.96	$3.94 \pm 0.16 \times 10^3$	8.82	$2.09 \pm 0.14 \times 10^3$	16.6
DFP	$3.75 \pm 0.24 \times 10^4$	0.94	$2.88 \pm 0.08 \times 10^4$	1.20	$1.10 \pm 0.11 \times 10^4$	3.15
CPO	$1.54 \pm 0.34 \times 10^5$	0.25	$1.71 \pm 0.29 \times 10^5$	0.21	$1.28 \pm 0.05 \times 10^4$	2.71

[a]Data displayed are mean ± SEM, $n \geq 3$. IC_{50} values were calculated using the equation $IC_{50}=\ln(2)/k_i \times t$ where time (t) is 20 min.
[b] MIP = mipafox; DFP = diisopropylphosphorofluoridate; CPO = chlorpyrifos oxon.
[c] R890H had significant reductions from *wt*NEST ($p<0.5$) for MIP and DFP
[d] M1012V had significant reductions from both *wt*NEST and R890H for all three inhibitors.

Table 4.3. Kinetic values of aging for neuropathy target esterase catalytic domain (NEST)[a]

Inhibitor[b]	k_4 (min^{-1})	$t_{1/2}$ (min)
MIP[c]	no reactivation	*n.d.*
DFP	0.112 ± 0.037	6.18
CPO	0.161 ± 0.044	4.30

[a] Data displayed are mean ± SEM, n = 3, The half-time of aging ($t_{1/2}$) = ln(2)/k_4.
[b] MIP = mipafox; DFP = diisopropylphosphorofluoridate; CPO = chlorpyrifos oxon.
[c] There was no reactivation for MIP-inhibited NEST at any time point, and $t_{1/2}$ could not be determined for mipafox (*n.d.*)

Table 4.4. Reported or calculated fixed-time IC_{50} values for neuropathy target esterase (NTE) or NTE catalytic domain (NEST)[a]

Inhibitor[b]	Reported IC_{50} values (μM) (median)	Reference
MIP	12 – 6.1 (7.7)	Lotti and Johnson, 1978[c] Ehrich *et al.*, 1997[d] Atkins and Glynn, 2000[e] Kropp and Richardson, 2003[f] Kropp *et al.,* 2004[g]
DFP	1.2 - 0.7 (0.84)	Lotti and Johnson, 1978 Ehrich *et al.,* 1997 Atkins and Glynn, 2000 Kropp *et al.,* 2004
CPO	0.35 – 0.069 (0.24)	Richardson *et al.,* 1993[h] Ehrich *et al.*, 1997 Kropp and Richardson, 2003

[a] IC_{50} values derived from the literature or calculated from reported bimolecular rates of inhibition (k_i) using the equation $IC_{50}=\ln(2)/k_i \times t$ where time (t) is 20 min.
[b] MIP = mipafox; DFP = diisopropylphosphorofluoridate; CPO = chlorpyrifos oxon.
[c] Lotti and Johnson reported 20 minute IC_{50} values derived from human and hen brain NTE.
[d] Ehrich *et al.* reported 30 minute IC_{50} values derived from neuroblastoma cell NTE.
[e] Atkins and Glynn reported 20 minute IC_{50} values derived both from hen brain homogenate NTE and NEST.
[f] Kropp and Richardson reported k_i values for NTE derived from hen brain homogenates.
[g] Kropp *et al.* reported k_i values derived from NEST.
h Richardson *et al.* reported k_i values derived from hen brain NTE.

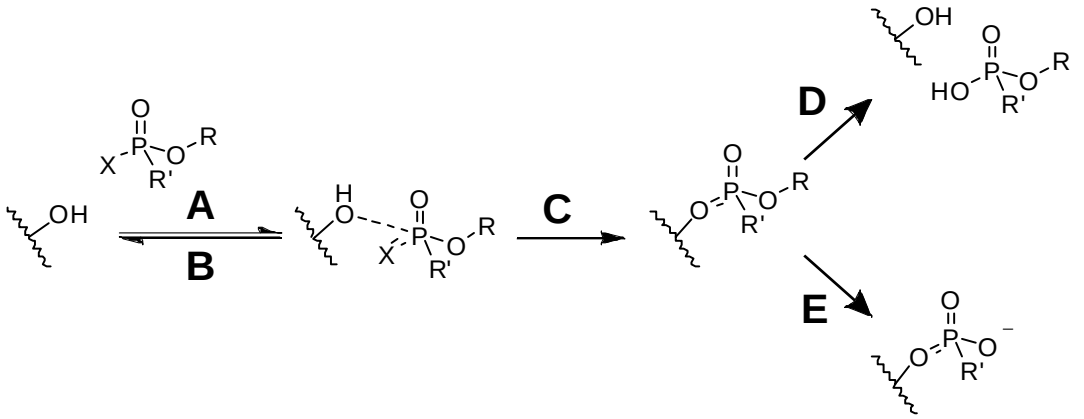

Figure 4.1. Interactions of OP compounds with serine esterases. As the OP comes in proximity to the esterase (A), there is a formation of the Michaelis-type complex, which is reversible (B). There is then a nucleophilic attack on the phosphorus (C), covalently binding the OP to the esterase. This entire forward process is described as inhibition. Post-inhibitory processes include reactivation, where there is a hydrolysis of the covalent bond (D), either spontaneously or catalyzed by oximes or KF, or aging, where there is cleavage of the bond (E), leaving a negative charge on the moiety.

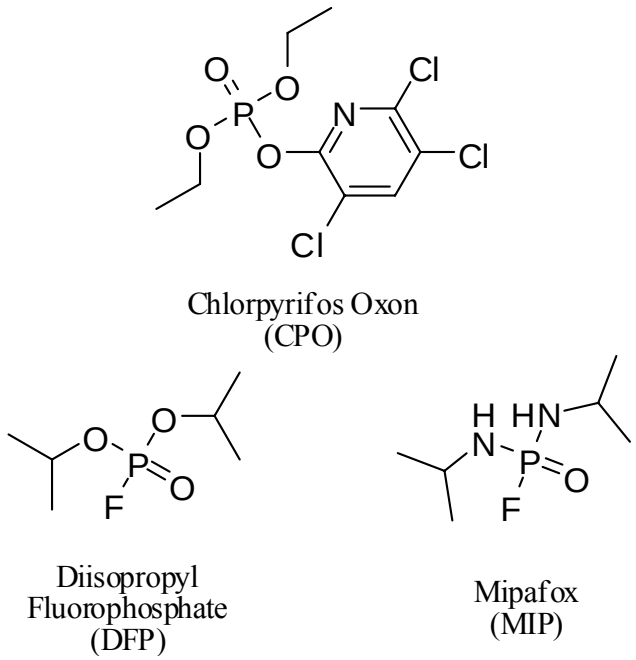

Figure 4.2. Chemical structures of inhibitors CPO, DFP, and MIP.

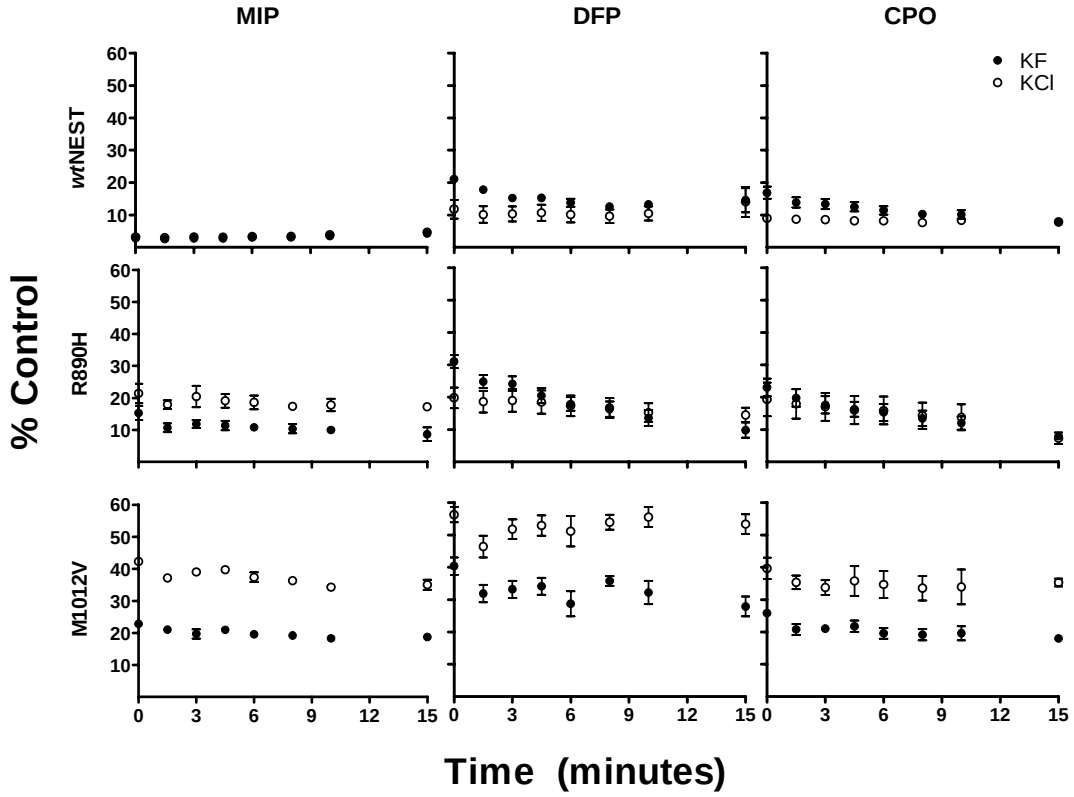

Figure 4.3. Residual activity of NEST. Values for each mutant and each inhibitor expressed as a percent of the uninhibited control. The top row is that of *wt*NEST, which aged as expected. The middle row shows R890H mutation, and the bottom row shows M1012V mutation. Values for KF reactivated species are shown by filled symbols (•) and those for KCl non-reactivated control species are shown as open symbols (○). Data are expressed as mean ± SEM, $n \geq 3$.

References

Aldridge, W.N., and Reiner, E. (1972). *Enzyme Inhibitors as Substrates: Interactions of Esterases with Esters of Organophosphorus and Carbamic Acids*. North-Holland Publishing, Amsterdam.

Akassoglou, K., Malester, B., Xu, J., Tessarollo, L., Rosenbluth, J., and Chao, M.V. (2004) Brain-specific deletion of neuropathy target esterase/swisscheese results in neurodegeneration. *PNAS.* **101,** 5075-5080.

Atkins, J., and Glynn, P. (2000). Membrane association of and critical residues in the catalytic domain of human neuropathy target esterase. *Biochem. J.* **275,** 24477-24483.

Beirowski, B., Adalbert, R., Wagner, D., Grumme, D.S., Addicks, K., Ribchester, R.R., and Coleman, M.P. (2005). The progressive nature of Wallerian degeneration in wild-type and slow Wallerian degeneration (Wld^S) nerves. BMC Neuroscience **6,** 6-32.

Clothier, B. and Johnson, M.K. (1979). Rapid aging of neurotoxic esterase after inhibition by di-isopropyl phosphorofluoridate. *Biochem. J.* **177,** 549-558.

Davis, C.S., and Richardson, R.J. (1980). Organophosphorus compounds, In *Experimental and Clinical Neurotoxicology* (Spencer, P.S., Schaumburg, H.H., eds.) pp. 527-544, Williams and Wilkins, Baltimore.

Erich, M., Correll, L., and Veronesi, B. (1997). Acetylcholinesterase and neuropathy target esterase inhibitions in neuroblastoma cells to distinguish organophosphorus compounds causing acute and delayed neurotoxicity. *Fundam. Appl. Toxicol.* **38,** 55-63.

Glynn, P. (2006). A mechanism for organophosphate-induced delayed neuropathy. *Toxicol. Lett.* **162,** 94-97.

Johnson, M.K. (1969). The delayed neurotoxic action of some organophosphorus compounds. Identification of the phosphorylation site as an esterase. *Biochem. J.* **114,** 711-717.

Johnson, M.K. (1977). Improved assay of neurotoxic esterase for screening organophosphates for delayed neurotoxicity potential. *Arch. Toxicol.* **37,** 113-115.

Jokanovic, M., Stepanovic, R.M., Maksimovic, M., Kosanovic, M., and Stojiljkovic, M.P. (1998). Modification of the rate of aging of diisopropylfluorophosphate-inhibited neuropathy target esterase of hen brain. *Toxicol. Lett.* **95**, 93-101.

Kayyali, U.S., Moore, T.B., Randall, J.C., and Richardson, R.J. (1991). Neurotoxic esterase (NTE) assay: Optimized conditions based on detergent-induced shifts in the phenol/4-aminoantipyrine chromophore spectrum. *J. Anal. Toxicol.* **15,** 86-89.

Kovarik, Z., Radic, Z., Berman, H.A., Simeon-Rudolf, V., Reiner, E., and Taylor, P. (2003). Acetylcholinesterase active centre and gorge conformations analysed by combinatorial mutations and enantiomeric phosphonates. *Biochem. J*

Kropp, T.J., Glynn, P., and Richardson, R.J. (2004). The mipafox-inhibited catalytic domain of human neuropathy target esterase ages by reversible proton loss. *Biochemistry* **43**, 3716-3722.

Kropp, T.J., and Richardson, R.J. (2003). Relative inhibitory potencies of chlorpyrifos oxon, chlorpyrifos methyl oxon, and mipafox for acetylcholinesterase versus neuropathy target esterase. *J. Toxicol. Environ. Health A* **66**, 1145-1157.

Lotti, M. and Johnson, M.K. (1978). Neurotoxicity of organophosphorus pesticides: Predictions can be based on in vitro studies with hen and human enzymes. *Arch. Toxicol.* **41,** 215-221.

Lotti, M. and Moretto, A. (2005). Organophosphate-induced delayed polyneuropathy. *Toxicol Rev.* **24,** 37-49.

Lush, M.J., Li, Y., Willis, A.C., and Glynn, P. (1998). Neuropathy target esterase and a homologous Drosophila neurodegeneration-associated mutant protein contain a novel domain conserved from bacteria to man. *Biochem. J.* **332,** 1-4.

Quistad, G.B., Barlow, C., Winrow, C.J., Sparks, S.E., and Casida, J.E. (2003). Evidence that mouse brain neuropathy target esterase is a lysophospholipase. *PNAS* **100,** 7983-7987.

Rainier, S., Bui, M., Mark, E., Thomas, D., Tokarz, D., Ming, L., Delaney, C., Richardson, R.J., Albers, J.W., Matsunami, N., Stevens, J., Coon, H., Leppert., M., and Fink, J. (2008). Neuropathy target esterase gene mutations cause motor neuron disease. *Am. J. Hum. Genet.* **82,** 780-785.

Richardson, R.J. (2005). Organophosphate poisoning, delayed neurotoxicity. In *Encyclopedia of Toxicology* (Wexler, P., ed.) pp 302-306, Academic Press, New York.

Richardson, R.J., Moore, T.B., Kayyali, U.S., Fowke, J.H., and Randall, J.C. (1993). Inhibition of hen brain acetylcholinesterase and neurotoxic esterase by chlorpyrifos in vivo and kinetics of inhibition by chlorpyrifos oxon in vitro: application to assessment of neuropathic risk. *Fundam. Appl. Toxicol.* **20**, 273-279.

van Tienhoven, M., Atkins, J., Li, Y., and Glynn, P. (2002). Human neuropathy target esterase catalyzes hydrolysis of membrane lipids. *J. Biol. Chem*. **277,** 20942-20948.

Vose, S.C., Fujioka, K., Gulevich, A.G., Lin, A.Y., Holland, N.T., and Casida, J.T. (2008). Cellular function of neuropathy target esterase in lysophophatidylcholine action. *Toxicol. Appl. Pharmacol.* **232,** 376-383.

Winrow, C.J., Hemming, M.L., Allen, D.M., Quistad, G.B., Casida, J.E., and Barlow, C. (2003). Loss of neuropathy target esterase in mice links organophosphate exposure to hyperactivity. *Nat. Genet.* **3,** 477-485.

CHAPTER 5

SUMMARY AND CONCLUSIONS

Conclusions

Organophosphorus (OP) compounds covalently and may irreversibly bind to serine hydrolases, and there are several pathologies associated with this interaction (Casida and Quistad, 2005). If they bind to acetylcholinesterase (AChE), the associated toxicity is due to the build up of acetylcholine (ACh) in the synapses of cholinergic neurons and consequent overstimulation (Thompson and Richardson, 2004). Although there is no toxicity associated with the loss of butyrylcholinesterase (BChE), this enzyme may be used as a scavenger or biomarker of OP toxicity (Nicolet *et al.* 2003). The molecular mechanism between exposure to organophosphorus (OP) compounds and the onset of the axonal degeneration characterizing OP induced delayed neurotoxicity (OPIDN) is poorly understood. It is recognized that the inhibition and subsequent aging of neuropathy target esterase (NTE) by neuropathic OP compounds is correlated with OPIDN; however, the molecular events following this initial interaction are unknown (Casida and Quistad, 2005).

Recently, NTE was discovered to be a lysophospholipase and to function *in vivo* to degrade lysophosphatidylcholine (LPC) to glycerophosphocholine (GPC) (Quistad *et*

al., 2003; Vose *et al.,* 2008). The cellular levels of LPC are tightly regulated by several hydrolases, and it has been shown that when mice are exposed to high levels of LPC, they develop extensive demyelination (Hall, 1972). Furthermore, the *Drosophila* homologue swisscheese (SWS) has shown to specifically bind with the C3-catalytic subunit of cAMP activated protein kinase (PKA-C3) (Bettencourt de Cruz *et al.,* 2008). By deleting SWS, PKA-C3 is uncontrolled, and the over expression of this kinase leads to a progressive neurodegeneration. This research indicates that NTE may also have the same binding mechanism and role in disease progression in humans.

The classic *in vivo* model of OPIDN is the hen, because of similarities of enzymological properties of the NTE and AChE enzymes and the alignment of clinical presentations of the axonal lesions with human intoxications. Several *in vitro* assays have been developed to improve the requirements for screening of OP compounds for OPIDN including recombinant protein, tissue homogenates, and cell lines (Atkins and Glynn, 2000, Ehrich *et al.,* 1997). In addition to chickens, *Drosophila*, mice, *C. elegans*, and yeast all have NTE homologues, and associated pathologies with the modifications of this protein, including a lack of glycerophosphocholine in yeast when NTE is deleted (Lush *et al.,* 1998). *In vivo* modeling the disease in rodents has proven to be difficult, since they require a much higher dose of compound to overcome metabolism and axonal length to develop classical OPIDN. Correlations have been made with inhibitory potencies of neuropathic and cholinergic OP compounds between species, but not for mechanism of disease.

The covalent binding of OP compounds to serine esterases usually involves a nucleophilic attack on phosphorus cleaving an electrophilic leaving group, commonly a

fluoride ion. The mechanism of inhibition and aging can be elucidated using protein mass spectrometry (MS) technology (Kropp *et al.,* 2004, Kropp and Richardson, 2006). In addition to inhibition data, MS data can reveal if the OP-enzyme complex does indeed undergo aging, an apparent requirement for OPIDN pathogenesis. Revealing this mechanism of inhibition by phosphylation and subsequent aging is an important task when unique OP compounds are designed, such as the fluorinated aminophosphonate (FAP) compounds to predict neuropathic potential.

Summary of Data Chapters

The phosphorylation of BChE by FAP compounds revealed through MS

The data collected by surface enhanced laser desorption/ionization time-of-flight mass spectroscopy (SELDI-TOF MS) in Chapter 2 showed that FAP compounds were found to inhibit BChE through phosphorylation of the active site serine, cleaving the carbon-phosphorus (C—P) bond, and subsequently aged through net dealkylation. Although FAP compounds were initially found to inhibit serine esterases, the covalent phosphorylation seemed unlikely, due to the chemical stability of the C—P bond (Makhaeva *et al.,* 2005; Quinn *et al.,* 2007). Crystallization studies leading into this work revealed that the generally nonreactive C—P bond was unusually long, due to the adjacent fluorinated carbon groups (Chekhlov *et al.,* 1995; Makhaeva *et al.,* 2005; Wijeyesakere *et al.,* 2008). This would make the bond more accessible to nucleophilic attack by the serine, and theoretically stabilize the leaving group.

Using horse serum BChE for the SELDI-TOF MS analysis of serine adducts was optimal, because OP adducts of this protein are well documented in the literature (Li *et al.,* 2007, Bartlilng *et al.,* 2007, Kropp and Richardson, 2007). Furthermore, spectra collected for trypsin digested uninhibited BChE have an easily identified peak corresponding to the average mass of the peptide containing the active site serine, and an absence of peaks in the range of predicted mass adducts. The calculated masses for inhibited adducts aligned with the observed mass shift peaks of the active site serine peptide for each of the FAP analogues, except in the case of the *n*-hexyl-FAP. Previous studies suggest that a longer alkyl chain significantly shortens the $t_{1/2}$ of aging by dealkylation for OP inhibited BChE (Masson *et al.,* 1997). Although no literature was found for this specific alkyl branching, other cyclohexyl and the pinacolyl substituted OP compounds age quickly (Masson *et al.,* 1997; Saxena *et al.,* 1998; Worek *et al.,* 1998; Bartling *et al.,* 2007). Given that the protocol requires an incubation of BChE with trypsin for at least three hours, it would be difficult to identify the inhibited adduct of a compound that ages much more rapidly.

There were observed mass shifts of aged adducts corresponding with the protonated predicted mass adduct sizes except for isobutyl. The negative charge left on the OP-serine aged adducts is probably protonated due to the acidic nature of the matrix, which contains trifluoroacetic acid and α-cyano-4-hydroxycinnamic acid. Other isobutyl substituted OP compounds had the same anomaly when analyzed by MS, including the isobutyl-ester analogue of Russian-VX and the isobutyl-ester analogue of sarin, despite having recorded kinetic values of aging. Moreover, a recent MS analysis of BChE-OP adducts revealed that adducts may be identified when the level of inhibition is as low as

3% (Sun and Lynn, 2007). Because aging was allowed to proceed for 72 hours, it could be hypothesized that OP-inhibited BChE is refractory to aging by isobutyl esters.

In addition to inhibitory data, protein MS proves to be a useful technology in identifying potential of unusual OP compounds, such as FAP compounds, to inhibit and age serine esterases, as supported by these data.

Assessment of delayed neurotoxic potential of OP compounds

Correlations between the bimolecular rates of inhibition (k_i) values for OP inhibited AChE and NTE and relative inhibitory potential (RIP, k_iAChE/k_iNTE) values, among mouse brains, human recombinant enzymes, and hen brains in Chapter 3 allow the accurate prediction of the potential of an OP compound to cause OPIDN. Each group of enzymes within the relative species were able to correctly predict whether the compound would elicit a predominantly cholinergic toxicity associated with the inhibition of AChE or have potential to cause OPIDN through a higher relative inhibition of NTE.

The k_i values reported in this research agreed with those that had been published in the literature (see Chapter 3 for references). The values for human recombinant proteins and mouse brain enzymes had strong correlation to the hen brain enzymes, which is considered the standard for OPIDN testing. The association of these values would indicate that for *in vitro* screening purposes the enzymes would give analogous results for potency of inhibitors for both NTE and AChE and for predicting neuropathic potential. Using human recombinant enzymes rather than enzymes from brain tissues would not only eliminate the need to house and sacrifice animals, but would make it easier to develop high throughput assays that could accurately determine the effectiveness and neuropathic potential of newly developed or untested OP compounds.

The kinetics of the postinhibitory reaction of aging, although not thoroughly investigated in this chapter, is also important in establishing correlations among the species. The aging data were collected with NEST for the three inhibitors, and the k_4 values agree with previously published data for both human recombinant and chicken brain enzymes. Although not understood why, OPIDN is currently believed to be initiated by the negatively charged moiety left on the NTE-OP complex after aging. It would be noteworthy to examine the rates of aging of AChE among the species to further correlate the kinetic properties among them. Although no additional toxicity is associated with the aging of AChE, the enzyme is refractory to reactivation limiting possible treatments.

Further experiments must be performed to complete the *in vitro* assessment of neuropathic compounds. The strong correlation of both NTE and AChE is an appropriate step towards developing an *in vivo* model. Before such a model could be developed, there would need to be further research in both the biotransformation of possible protoxicants and metabolism of the OP compounds. Furthermore, although mice display a type of delayed neurotoxicity, it would be important to establish histopathological changes within the nerve tissue to further correlate OPIDN in the mouse model.

Altered kinetic properties of mutations found in NTE-motor neuron disease

Three mutations were found in NTE in patients with a hereditary spastic paraplegia, named NTE-related motor neuron disease (NTE-MND) (Rainier *et al.,* 2008). Two of these mutations, arginine 890 to histidine, and methionine 1012 to valine (M1012V), were created in NEST and found to have altered enzymatic properties. The first of the changes in enzymatic properties was a significant reduction in the hydrolysis

of the exogenous substrate phenyl valerate. Deletion of NTE creates an embryonic lethal phenotype, and OPIDN is associated with the inhibition and aging of >80% of NTE in mice (Moser *et al.,* 2004; Akassoglou, 2004). A hyperactivity phenotype is associated with sustained reduced (but not abolished) NTE activity whether induced by a heterozygous knockout mutation ($nte^{+/-}$) or by sustained inhibition by a neuropathic compound (Winrow *et al.,* 2003). It should be noted that this phenotype does not occur with chronic dosing of compounds incapable of aging.

There was also reduction in the k_i values for the two inhibitors DFP and MIP in both mutations, and a marked reduction for the CPO-inhibited M1012V mutation. Moreover, the NTE-MND mutations had a distorted postinhibitory reaction. While values for k_4 were calculated for *wt*NEST, this was not possible for the mutant enzymes. This is because the residual activity for the non-reactivated species was actually higher than the residual activity for the reactivated species. Mutations in inhibitory profile have not been shown in NTE, however, they have been investigated in AChE, and certain mutations do alter inhibitory specificity (Kovarik *et al.,* 2003).

Significance and further investigations

Phosphorylation by FAP compounds

The data collected from Chapter 2 reveal that the FAP compounds indeed phosphorylate BChE through a scission in the C—P bond. It would be useful to continue this work with other serine esterases. This is especially true for the isobutyl- and *n*-hexyl-FAP analogues, because there were no identified aged or inhibited peaks (respectively).

Collecting a complete set of bimolecular rate constants of inhibition for human recombinant AChE and NTE would allow for the calculation of RIP values, and a correlation between the alkyl group and neuropathic potential of these compounds may be made. Experimentally determining the post-inhibitory rates of reactivation and aging would help to further characterize these compounds.

Moreover, while performing the research with the FAP compounds, a type of solvent effect was discovered. As the compounds stood for increasing times in organic solvent, the inhibitory potency increased dramatically (data not shown). This was more pronounced in acetone than in DMSO. In addition to having a labile C—P bond, crystallographic studies revealed that these compounds exist in dimers. From preliminary observations, one could hypothesize that dilutions of these compounds in solvents solvents, as well as variations in concentrations and temperatures, could have an effect on the percentage of compound that exists in dimeric form. Furthermore, it could also be stated, that the dimer hinders the nucleophilic attack on the phosphorus by sterically blocking access to the active site. Infrared studies could be performed with the compounds in several different organic solvents to determine if there is a dimer to monomer transformation by viewing a change in the resonance of the hydrogen bonded species.

Assay development for prediction of neuropathic potential

Although the data presented in Chapter 3 provide strong evidence of a correlation among chicken, mice, and human enzymes, further testing should be performed before

replacing the standard assay. Several different experiments could be performed to better characterize a model.

Additional inhibitors could be characterized, to strengthen (or weaken) the correlation across species. Although there are values reported in the literature, aging experiments could further correlate the rates of postinhibitory reactions between the species. One problem with comparing literature values is that the conditions by which the data are collected often vary in enzyme preparation, temperature, pH, and incubation time. Collecting data on compounds in consistent conditions could be more useful in comparing the enzymological properties of the homologous proteins. A series of compounds such as the FAP compounds would provide an excellent set of data to compare not only kinetic rates, but identify trends in affect of alkyl chain length within each species.

An ideal outcome of the *in vitro* modeling would be to generate an *in vivo* mouse model to test the neuropathic compounds. Characterizing the kinetic profiles of the red blood cell AChE and lymphocyte NTE in mice and humans would strengthen this model, because it could provide a tissue specific species correlation. Furthermore, metabolic activation of potential protoxicants should be developed, such as human liver microsomal preparation, because of differences in the metabolism of OP compounds among the species. Furthermore, the distribution and elimination of the compounds should be studied in *ex-vivo* studies to determine these system of the OP compounds.

NTE-related motor neuron disease mutations

The data collected from the NTE-MND mutations in human recombinant NEST were quite significant, because the mutant proteins had significant differences in

enzymological properties. The reduction in catalytic hydrolysis of phenyl valerate and in the kinetics of inhibition show that, although not profound, these mutations affect the appropriate enzymological function. Creating these mutations in a mouse model and comparing the pathology to the hyperactive phenotype found in association with the heterozygous ($nte^{+/-}$) mouse would reinforce the connection between the mutants and the disease state. Furthermore, it would be interesting to see the effect on *in vivo* inhibitor potency. One may conclude that the NTE-MND mice would be more sensitive to inhibitors due to a lowered specific NTE activity; however, the enzyme itself is altered. Not only are the kinetic values of inhibition decreased in these mutations, but the kinetic of aging are distorted. These alterations in enzymatic properties demonstrate a possible correlation between a change in the catalytic domain of NTE and the NTE-MND disease itself.

References

Akassoglou, K., Malester, B., Xu, J., Tessarollo, L., Rosenbluth, J., and Chao, M.V. (2004) Brain-specific deletion of neuropathy target esterase/swisscheese results in neurodegeneration. *PNAS.* **101,** 5075-5080.

Atkins, J., and Glynn, P. (2000). Membrane association of and critical residues in the catalytic domain of human neuropathy target esterase. *J. Biol. Chem*. **275**, 24477-24483.

Bartling, A., Worek, F., Szinicz, L., and Thiermann, H. (2007). Enzyme-kinetic investigation of different sarin analogues reacting with human acetylcholinesterase and butyrylcholinesterase. *Toxicology* **233,** 166-172.

Bettencourt da Cruz, A., Wentzell, J., and Kretzschmar, D. (2008) Swiss cheese, a protein involved in progressive neurodegeneration, acts as a noncanonical regulatory subunit for PKA-C3. *J. Neurosci*. **28,** 10885-10892.

Casida, J.E. and Quistad, G.B. (2005). Serine hydrolase targets of organophosphorus toxicants. *Chem.-Biol. Int.* **157-158,** 277-283.

Chekhlov, A.N., Aksinenko, A.Y., Sokolov, V.B., and Martynov, I.V. (1995). Crystal and molecular structure and synthesis of O,O-Diisopenytl-1-benzenesulfonamido-1-trifuoromethyl-2,2,2-trifuoroethylphosphonate. *Dokl. Chem.* **345,** 296.

Ehrich, M., Correll, L., Veronesi, B. (1997). Acetylcholinesterase and neuropathy target esterase inhibitions in neuroblastoma cells to distinguish organophosphorus compounds causing acute and delayed neurotoxicity. *Fund. Appl. Toxicol.* **38,** 55-63.

Hall, S.M. (1972). The effect of injections of lysophosphatidyl choline into white matter of the adult mouse spinal cord. *J. Cell Sci.* **10,** 535-546.

Johnson, M.K. (1982). The target for initiation of delayed neurotoxicity by organophosphorus esters: biochemical studies and toxicological applications. *Rev. Biochem. Toxicol.* **4,** 141-212.

Kropp, T. J., Glynn, P., and Richardson, R. J. (2004). The mipafox-inhibited catalytic domain of human neuropathy target esterase ages by reversible proton loss. *Biochemistry* **43**, 3716-3722.

Kropp, T.J., and Richardson, R.J. (2006). Aging of mipafox-inhibited human acetylcholinesterase proceeds by displacement of both isopropylamine groups to yield a phosphate adduct. *Chem. Res. Toxicol*. **19**, 334-339.

Lush, M.J., Li, Y., Willis, A.C., and Glynn, P. (1998). Neuropathy target esterase and a homologous *Drosophila* neurodegeneration-associated mutant protein contain a novel domain conserved from bacteria to man. *Biochem. J.* **332,** 1-4.

Makhaeva, G.F., Malygin, V.V., Aksinenko, A.Y., Sokolov, V.B., Strakhova, N.N., Rasdolsky, A.N., Richardson, R.J., and Martynov, I.V. (2005). Fluorinated α-aminophosphonates – a new type of irreversible inhibitors of serine hydrolases. *Dokl. Biochem. Biophys.* **400**, 831-835.

Masson, P., Fortier, P.L., Albaret, C., Froment, M.T., Bartels, C.F., and Lockridge, O. (1997). Aging of di-isopropyl-phosphorylated human butyrylcholinesterase. *Biochem J.* **327,** 601-607.

Moser, M., Yong, L., Vaupel, K., Kretzschmar, D., Kluge, R., Glynn, P., and Buettner, R. (2004). Placental failure and impaired vasculogenesis result in embryonic lethality for neuropathy target esterase-deficient mice. *Molec. Cell Biol.* **24,** 1667-1679.

Nicolet, Y., Lockridge, O., Masson, P., Fontecella-Camps, J.C., and Nachon, F. (2003). Crystal structure of human butyrylcholinesterase and of its complexes with substrate and products. *J. Biol. Chem.* **42,** 41141-41147.

Quinn, J.P., Kulakova, A.N., Cooley, N.A., and McGrath, J.W. (2007). New ways to break an old bond: the bacterial carbon-phosphorus hydrolases and their role in biochemical phosphorus cycling. *Environ. Microbiol.* **9,** 2392-2400.

Quistad, G.B., Barlow, C., Winrow, C.J., Sparks, S.E., and Casida, J.E. (2003). Evidence that mouse brain neuropathy target esterase is a lysophospholipase. *PNAS* **100,** 7983-7987.

Rainier, S., Bui, M., Mark, E., Thomas, D., Tokarz, D., Ming, L., Delaney, C., Richardson, R.J., Albers, J.W., Matsunami, N., Stevens, J., Coon, H., Leppert., M., and Fink, J. (2008). Neuropathy target esterase gene mutations cause motor neuron disease. *Am. J. Hum. Genet.* **82,** 780-785.

Saxena, A., Viragh, C., Frazier, D.S., Kovach, I.M., Maxwell, D.M., Lockridge, O. and Doctor, B.P. (1998). The pH dependence of dealkylation in soman-inhibited cholinesterases and their mutants: further evidence for a push-pull mechanism. *Biochemistry* **39,** 15086-15096.

Sun, J. and Lynn, B.C. (2007). Development of a MALDI-TOF-MS method to identify and quantify butyrylcholinesterase inhibition resulting from exposure to organophosphate and carbamate pesticides. *J. Am. Soc. Mass Spectrom.* **18,** 698-706.

Thompson, C.M. and Richardson, R.J. (2004). Anticholinesterase Insecticides. *Pesticide Toxicology and International Regulation* (T. Marrs and B. Ballantyne, Eds.) John Wiley and Sons, Ltd., Chester. pp. 89-127.

Vose, S.C., Fujioka, K., Gulevich, A.G., Lin, A.Y., Holland, N.T., and Casida, J.T. (2008). Cellular function of neuropathy target esterase in lysophophatidylcholine action. *Toxicol. Appl. Pharmacol.* **232,** 376-383.

Wijeyesakere, S.J., Nasser, F.A, Kampf, J.W., Aksinenko, A.Y., Sokolav, V.B., Malygin, V.V., Makhaeva, G.F., and Richardson, R.J. (2008). Diethyl [2,2,2-trifluoro-1-phenylsulfonylamino-1-(trifluoromethyl)ethyl]phosphonate. *Acta Cryst.* **E65**, o1425-o1426.

Winrow, C.J., Hemming, M.L., Allen, D.M., Quistad, G.B., Casida, J.E., and Barlow, C. (2003). Loss of neuropathy target esterase in mice links organophosphate exposure to hyperactivity. *Nat. Genet.* **33,** 477-485.

Worek, F., Diepold, C., and Eyer, P. (1999). Dimethylphosphoryl-inhibited human cholinesterasese: inhibition, reactivation, and aging kinetics. *Arch. Toxicol.* **73,** 7-14.